HETEK

Control of Early Age Cracking in Concrete
Phase 3: Creep in Concrete

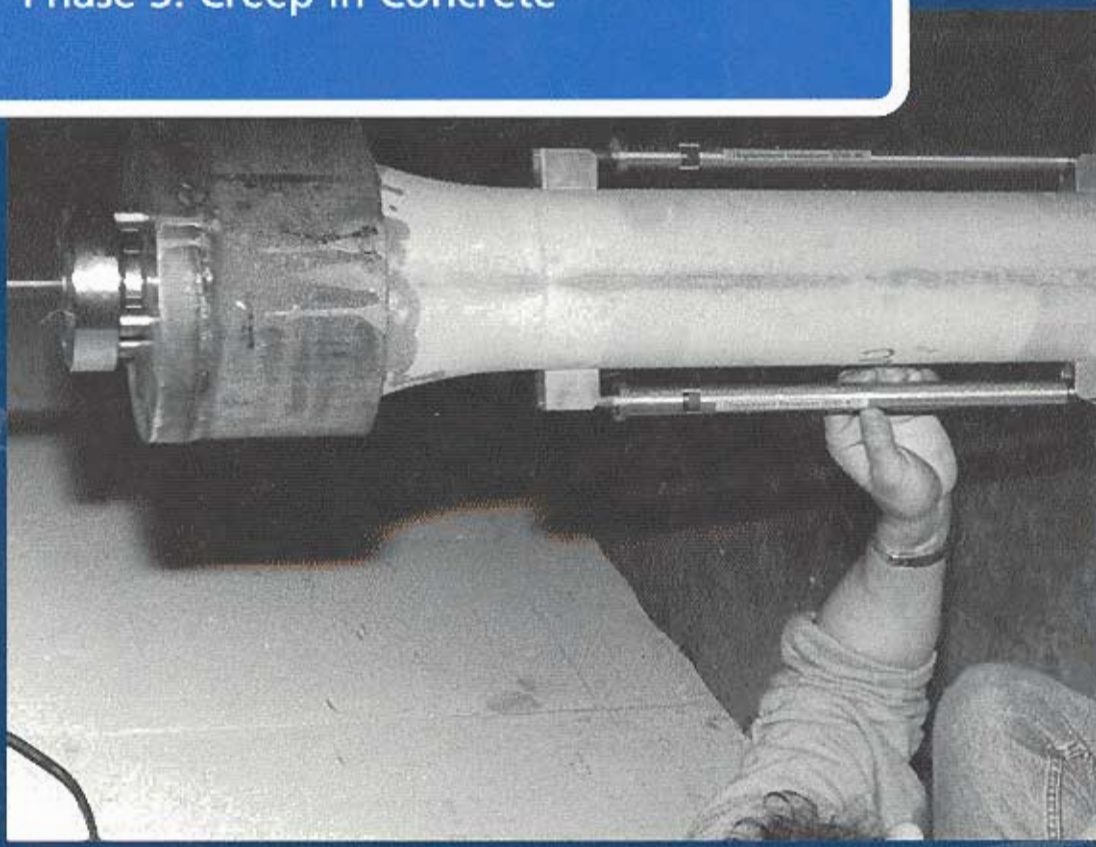

Report No.111
1997

Road Directorate Denmark Ministry of Transport

IRRD Information

Title in English	**HETEK -Control of Early Age Cracking in Concrete - Phase 3: Creep in Concrete**
Title in Danish	**HETEK -Styring af revner i ung beton - Fase 3: Krybning i Beton**
Authors	Anders Boe Hauggaard, Lars Damkilde, Per Freiesleben Hansen, Jacob Haugaard Hansen, Anders Nielsen and Søren Lolk Christensen
Subject classification	Field 32 Concrete

Key words

Concrete	4755
Analysis	7152
Material	4555
Numerical	6432
Properties	5925
Thermal stress in material	5575
Denmark	8028

Abstract

The mechancial properties of the "Road Directorate Concrete" at early ages are studied. Creep in tension at 24 and 72 maturity hours are measured on "dogbone" specimens. The development of tensile modulus of elasticity and strength are measured with a method developed here. The results are compared to compression values and splitting strengths. It is found that the properties of creep in tension are similar to the properites in compression. Further, the influence from temperature on creep is found to be significant.

UDK 691.32
620.191.33

ISSN 0909-4288

ISBN 87-7491-824-9

Contents

1 Introduction **1**

1.1 Creep of Early Age Concrete 1

1.2 Test Program for the Properties 3

1.3 Test Program for Creep 4

2 Measurement Technique **6**

2.1 Elastic Modulus and Strength 6

2.1.1 Tension 6

2.1.2 Compression 10

2.2 Creep and Relaxation 11

2.2.1 Developed Specimen 11

2.2.2 Loading Rig for the 20°C Tests 13

2.2.3 Loading Rig for the 40°C Tests 14

3 Results **17**

3.1 Tensile Properties at 20°C 17

3.1.1 Modulus of Elasticity and Tensile Strength 17

3.2 Tensile Properties at 40°C 18

3.2.1 Modulus of Elasticity and Tensile Strength 18

3.3 Tensile Properties, Discussion 20

3.3.1 Modulus of Elasticity 20

3.3.2 Tensile Strength 21

3.4 Tensile Properties, Creep at 20°C 23

3.4.1 Age at Loading 24 hours 23

3.4.2 Age at Loading 72 hours 25

3.4.3 Discussion 27

3.5 Compressive Properties at 20°C 28

3.5.1 Modulus of Elasticity and Compressive Strength 28

3.6 Compressive Properties at 40°C 29

3.6.1 Modulus of Elasticity and Compressive Strength 29

3.7 Compressive Properties, Discussion 30
3.7.1 Modulus of Elasticity 30
3.7.2 Compressive Strength 31
3.8 Compressive Creep, Age at Loading 24 hours 31
3.8.1 Loading History 31
3.8.2 Temperature History 32
3.8.3 Creep 33
3.9 Compressive Relaxation, Age at Loading 24 hours 34
3.10 Comparison of Modulus of Elasticity in Tension and Compression 35

4 Conclusion **37**

A Appendix **41**
A.1 Tensile strength and modulus of elasticity at $20°C$. 41
A.2 Splitting tensile strength at $20°C$. 42
A.3 Tensile strength and modulus of elasticity at $40°C$. 43
A.4 Splitting tensile strength at $40°C$. 44

B Appendix **45**
B.1 Compressive strength and modulus of elasticity at $20°C$. 45
B.2 Compressive strength and modulus of elasticity at $40°C$. 46

C Appendix **47**
C.1 Measured creep in Tension, Age at Loading 1 day 47
C.1.1 40% Load level, Creep vs. Time, Specimen 1 47
C.1.2 40% Load level, Creep vs. Time, Specimen 2 48
C.1.3 40% Load level, Shrinkage and Temperature vs. Time 49
C.1.4 60% Load level, Creep vs. Time, Specimen 1 and 2 50
C.1.5 60% Load level, Shrinkage and Temperature vs. Time 51
C.1.6 80% Load level, Creep vs. Time, Specimen 2 52
C.1.7 80% Load level, Shrinkage and Temperature vs. Time 53
C.2 Measured creep in Tension, Age at Loading 3 day 54
C.2.1 40% Load level, Creep vs. Time, Specimen 1 and 2 54
C.2.2 40% Load level, Shrinkage and Temperature vs. Time 55
C.2.3 60% Load level, Creep vs. Time, Specimen 1 and 2 56
C.2.4 60% Load level, Shrinkage and Temperature vs. Time 57

D Appendix **58**
D.1 Measured creep in Compression 58
D.1.1 40% Load level, $24°C$, Creep and Shrinkage vs. Time 58

D.1.2 40% Load level, 24°C, Temperature vs. Time 59
D.1.3 40% Load level, 40°C, Creep, Shrinkage and Temperature vs. Time 60
D.1.4 40% Load level, 20-40-20°C, Creep, Shrinkage and Temperature vs. Time 61

E Appendix **62**
E.1 Experimental Program on Creep in Tension 62
E.2 Experimental Program on Creep in Compression 63

Preface

This project on control of early age cracking is a part of the Danish Road Directorates research program, High Performance Concrete – The Contractors Technology, [1] abbreviated to HETEK.

In this program high performance concrete is defined as concrete with a service life in excess of 100 years in an aggressive environment.

The research program includes investigations concerning the contractors design of high performance concrete and execution of the concrete work with reference to the required service life of 100 years.

The total HETEK research program is divided into segment parts with the following topics:

- chloride penetration
- frost resistance
- control of early age cracking
- compaction
- curing, evaporation protection
- trial casting
- repair of defects

The Danish Road Directorate invited tenders for this research program which is mainly financed by the Danish Ministry for Commerce and Industry – The Commision of Research and Development Contracts.

The present report refers to the part of the HETEK project which deals with control of early age cracking.

For Durability reasons reinforced structural members should be well protected against penetration of water, chloride etc. This means that cracks should be avoided or at least the crack-width limited. Formation of cracks can take place already during the hardening process. An evaluation of the risk of crack formation involves a stress analysis. In stress analysis of hardening concrete structures, the load consists of the difference in thermal strains that arise from the heat of hydration. The mechanical properties, including autogenous shrinkage, of the concrete also change during the hardening process. If a stress analysis shows high stresses compared to the tensile strength there is a high risk of crack formation.

The purpose of this project is to investigate these effects and to prepare a guideline regarding Control of Early Age Cracking.

The project was carried out by a consortium consisting of:

Danish Concrete Institute represented by:

[1] In Danish: Højkvalitetsbeton – Entreprenørens Teknologi

- Højgaard & Schultz A/S
- Monberg & Thorsen A/S
- Rambøll
- COWI

and Danish Technological Institute, represented by the Concrete Center and Technical University of Denmark, represented by the Department of Structural Engineering and Materials.

Two external consultants, Professor Per Freiesleben Hansen and manager Jens Frandsen, are connected with the consortium.

The present report on creep in concrete has been carried out at the Technical University of Denmark.

Chapter 1

Introduction

1.1 Creep of Early Age Concrete

The time dependent properties of concrete has effect on several factors of interest when designing structures such as

- the risk of cracking
- the magnitude of deformations
- the redistribution of stresses

In the present context creep and relaxation of concrete is the issue and we denote both phenomena with creep. In relation to cracking creep reduces the stress singularities and thereby reduces the risk of cracking which is an advantage. However, creep at very early ages in the heating period may be a disadvantage because the compressive stresses are reduced. The influence of these stresses are as a buffer since the tensile stress changes generated by cooling have to offset the compressive stresses before tensile stresses appear. In practice tensile stresses are often starting to build up after about three days of hydration. The significance of creep is also seen by the increase in deformations in time. The instantaneous deformations upon loading may be only a fraction, e.g. 1/3, of the deformations after long time due to creep. Generally the stresses are redistributed in the structure by creep and this means that highly stressed areas are relieved on the expense of less stressed areas.
The development of creep is influenced by

- the age of the concrete
- the magnitude of stress
- the temperature
- the development of the moisture distribution

- the mix-proportions

The rate of creep decreases with age due to the progress of hydration. However also hardened concrete shows a decrease in the rate of creep with time and this indicates that other processes than hydration may be active, e.g. [3]. An example of such processes could be the interaction between moisture and solid cement gel due to adsorption effects.

Information about creep of concrete in tension, e.g. whether it is equal to creep in compression, is rather scarce. Further it is not clear if the non-linearity in creep observed at high compressive stress levels shown in Fig. 1.1, apply for tensile loading too.

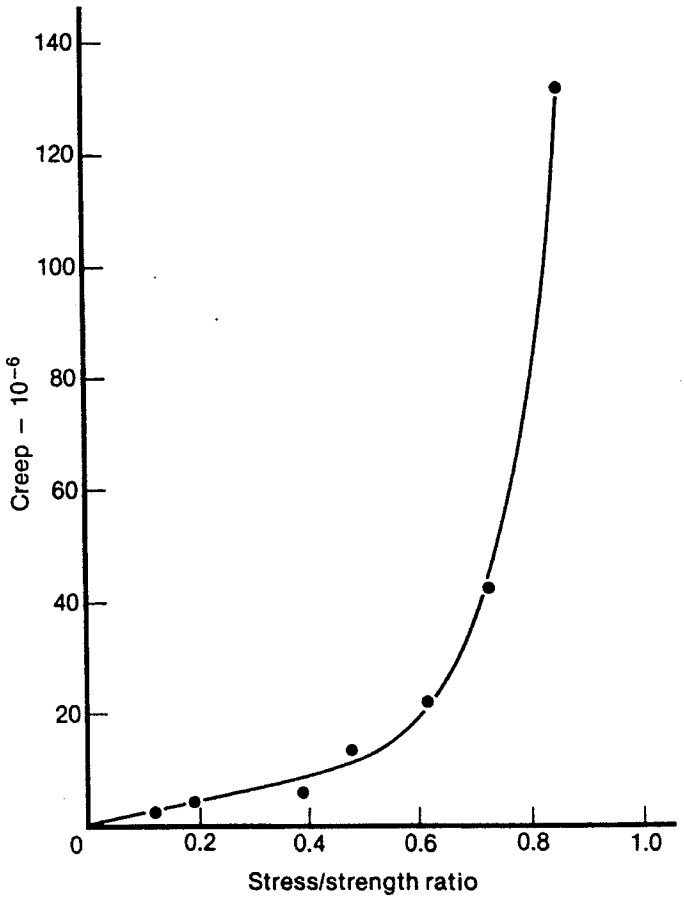

Figure 1.1: Non-linearity of creep in compression, [13].

Fig. 1.1 shows the amount of creep after one minute of loading as a function of the relative stress-level. The age at loading was 5 days. For relative loadings below about 50% the magnitude of creep seems to be linear whereas a large non-linear increase takes place at higher loadings. Normally the compressive loading is below 50% in structures and therefore the non-linearity is of little importance here. However when the loading is tensile and close to the tensile strength, as in the case of cracking, the non-linearity may have significant influence on the structural response. The behavior of hardened concrete under tension was the subject in [1]. The concrete was loaded to various constant sustained tensile load-levels and the time to failure was recorded. For relative loadings above 0.6 the concrete were

creeping until failure and the time before failure decreased significantly with an increase in loading. Below 0.6 there was no failure observed. A similar analysis in compression was made in [15] and here the shift in behavior occured at a relative load-level of about 0.7. The difference in load level where the shift takes place may be due to different definitions of the strength values. In [1] a special one-dimensional test equipment was used and in [15] prisms were loaded in compression.

During hydration the temperature increases and experiments, [18], indicate that this has influence on the magnitude of creep. An increase in isotherm temperature, in degrees $^{\circ}C$, with a factor two thus increases the creep with about 30%. Further the development of the moisture distribution influences creep and this is shown e.g. in [14]. Completely dry concrete concrete only creeps about 10% of completely saturated concrete.

Other factors related to the mix-proportions such as addition of admixtures and the type of aggregate also influence the creep properties. However, this is not the scope in the present context where one mix is studied.

1.2 Test Program for the Properties

The interest here in relation to the properties of early age concrete may be summerised to

- is the modulus of elasticity in tension equal to the one in compression?
- is the development of the tensile strength given by the splitting strength?
- does the maturity concept apply for the development of the modulus of elasticity, both in compression and in tension?

Normally it is assumed that the modulus of elasticity in tension is equal to the modulus of elasticity in compression and experiments are carried out to find out if this is a reasonable assumption. Further little information is available about the influence of the stress level on the modulus of elasticity in tension. Therefore dogbone shaped specimens have been designed to obtain the elastic modulus in tension. In compression the standard of cylinders are used to measure the elastic modulus. The experiments indicate, that the modulus of elasticity in tension is equal to the one in compression. For the stress levels tested, 45% and 60% of the tensile strength, no difference in the tensile modulus of elasticity was observed.

The dogbone shaped specimens are also used to measure the development of the one-dimensional tensile strength and these results are compared with the development of the splitting tensile strength. The specimen are cured in plastic bags after about 18 hours of hydration in the moulds. It is found that the one-dimensional tensile strength may exceed the splitting strength before about 14 days of hydration at $20^{\circ}C$ whereas the opposite holds for later terms.

The development of the compressive strength is measured using cylinders which have been sealed during curing in plastic bags in a tempered water bath. The development of the strengths are used in the loading of the creep experiments described next.

Both the elastic moduli and the strengths are determined at the temperature levels 20 and $40^{\circ}C$ and it is verified that the maturity concept is applicable.

1.3 Test Program for Creep

The scope with the creep test program is

- compare creep in tension and compression
- investigate whether non-linearities appear in tensile creep
- investigate the influence of temperature levels and gradients in time on the creep properties
- study relaxation

The program consists of a tensile part and a compressive part. In compression creep is measured during three temperature histories which are

- isotherm temperature of $20°C$
- isotherm temperature of $40°C$
- a 20–40–20$°C$ cycle

The age at first loading is 24 hours after mixing. Furthermore relaxation is measured in compression at $20°C$ after 72 hours of hydration and this is chosen to coincide with the time when tensile stress changes appear in practice. A compressive relaxation test is also carried out where the specimen is locked and heated. For all compressive tests the wanted load-level is 40% of the compressive strength. Since the strength develops in the period of testing, adjustment of the load-level is made with intervals of 24 hours. At each adjustment the compressive stress-level is increased to 40% of the actual strength. The age at loading in the compressive creep test at $40°C$ is 8 hours which correspond to about 20 maturity hours. The compressive testing program carried out is summerised in Table 1.1 and in Appendix E.1.

	Creep			Relaxation	
Temperature, $°C$	20	40	20-40-20	20	20-40-20
Specimen, numbers	2	2	2	2	2
Age at loading, hours	24	8	24	72	24

Table 1.1: Experiments carried out in compression.

Table 1.1 also shows the number of specimens used in each test and one of these is an unloaded dummy. The measurements of creep at different temperature histories show that the influence of gradients in time on the creep properties are significant.

The scope with the tensile program is to analyse the linearity to investigate whether it is possible to find a load level where a shift in behavior takes place similar to [1] and [15]. Further the magnitude of creep in tension is compared to the magnitude in compression.

The temperature is kept constant at about $20°C$ and two different ages at loading have been chosen which are 24 and 72 hours of hydration respectively. The experiments carried out in tension are summerised in Table 1.2 and in Appendix E.2.

	Age at loading	
Load level, %	24 hours	72 hours
40	3	3
60	3	3
80	2	x

Table 1.2: Experiments carried out in tension.

For each age at loading three relative tensile load-levels, 40%, 60% and 80%, are used and the load adjustment is made as in the case of compression. As shown each experiment consists of three specimens which are two loaded and one unloaded dummy.

In the experiments the loaded and unloaded specimens are kept together, as far as possible, during the hydration process to strive towards the same temperature development during the entire hydration period. Then the deformations measured on the dummy correspond to shrinkage and thermal deformations. These are used in the creep experiments to isolate the load induced deformation. In the first relaxation test at constant temperature $20°C$ the prescribed deformations are compensated with shrinkage and thermal deformations from the dummy during the test. In the second relaxation experiment the specimen is locked in the test machine and heated to induce compressive stresses. The results show that creep in tension is of the same order of magnitude as creep in compression. Further a non-linearity in tension was observed at the 80% load level.

Chapter 2

Measurement Technique

The moisture content in the aggregate is measured before mixing and the mix-proportions corrected accordingly. Due to limitations in the casting volume the specimens are cast in several batches. However, the concrete was mixed in the laboratory so differences between batches are assumed to be insignificant.

2.1 Elastic Modulus and Strength

2.1.1 Tension

Experimental Equipment

The development of the tensile strength and the modulus of elasticity are needed from 24 hours of hydration and onwards for loading in the creep tests. Dogbone shaped specimens have been developed for the measurements and they are described next.

The key-point in tensile strength tests is to establish a stress state close to uniform tension and then increase the stress level until failure. The recorded failure load is then distributed over the cross section to give an apparent tensile strength of the material. For control of that the failure takes place at a location where the area of the cross section is well-defined and the stress state is not influenced by end effects some sort of notch or dogbone shape are often used. In the present context the dogbone shape shown in Fig. 2.1 has been chosen and the specimen is shown placed in the testing machine both before and after the test. The dimensions of the specimens are

- length: 480 mm, body section: 200 mm
- area: 140 mm $\times$ 140 mm, body section: 100 mm $\times$ 100 mm
- glue thickness: 5 mm on the sides and no glue on the bottom

The zones between the ends and the body section, where the area changes, have a height of 60 mm and the shape of a circular arch with a diameter of 125 mm. At the corners the edges of the body section are tangential to the arch to reduce the stress increase due to

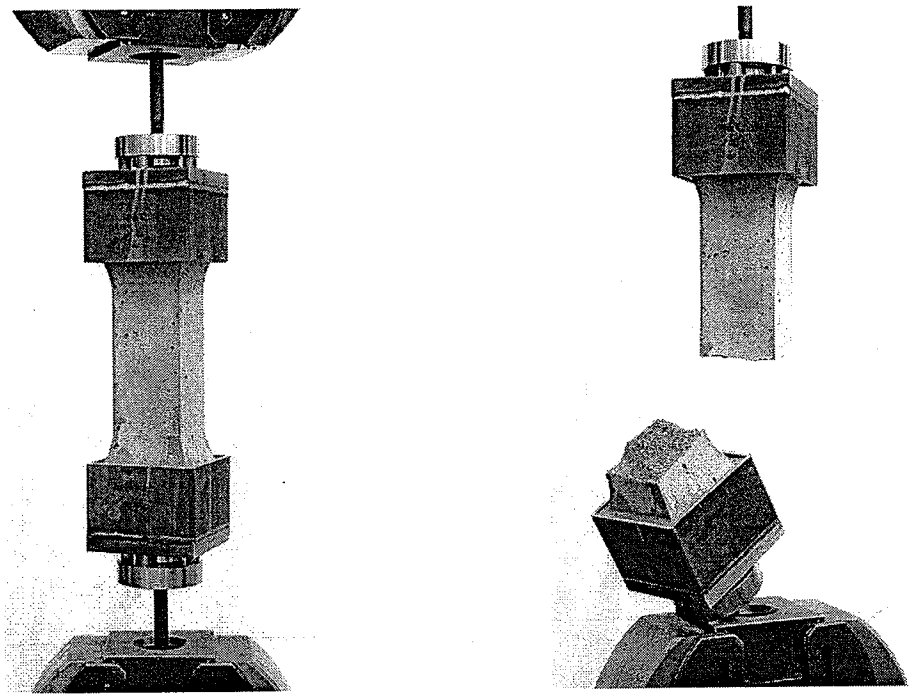

Figure 2.1: One-dimensional dogbone test specimen for the measurements of tensile modulus of elasticity and strength.

the change in area. The areas are chosen corresponding to a reduction factor of 2 and the dimension of the body section are specified to 4 times the maximum nominal aggregate size, d_{max}, by a standard, [21]. The thickness of the glue layer is specified by the manufacturer, [8], to a minimum of 5 mm and this is fulfilled in the test. There are little glue on the bottom of the cups and this means that the primary load is transfered through shear to the specimen.

The walls of the steel cups have a thickness of 5 mm and they are cut from a rectangular pipe into slices with a height of 100 mm. A plate with the thickness 25 mm has been welded to the end of the slices and 4 threads are made in the plate. The cups are cleaned after the test by burning out the glue. As seen in Fig. 2.1 the loading heads, which consists of a frictionless hinge, are bolted to the cups and fastened in the testing machine. These hinges have their center of rotation at the end surface of the specimen and thus reduces bending in the specimen. The loading heads make un- and reloading possible during the test and then the tensile modulus of elasticity may also be obtained simultaneously on the same specimen before pulling to failure.

One end of the specimen is glued at a time and the specimen is placed in the center of the cup and glue is flowed into the split between concrete surface and cup. The glue hardens within about one hour and then the other end is glued. The glue fasten both on wet and dry surfaces which is necessary for the earliest test. The glue chosen for this experiment and for the creep experiments described below is a two-component type, [8]. This was found after a broad investigation of many glue types. The recorded failure load is distributed over the cross-section of the body to yield the tensile strength.

The results obtained with the proposed one-dimensional testing procedure has been com-

pared with results obtained using the splitting tensile strength procedure. Since the splitting test is a standard, [2], it is only briefly described here and Fig. 2.2 shows a specimen after testing.

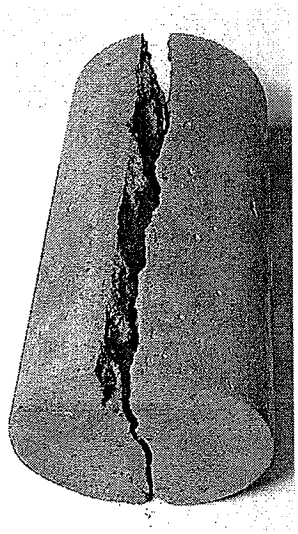

Figure 2.2: Standard splitting specimen.

The dimensions in the present context were chosen to a length, l = 300 mm, and a diameter, d = 150 mm. The procedure is to load the specimen along two opposite perimeters through a thin wood insert between the concrete and steel loading heads, [2]. At failure a crack in the load direction is formed as shown in Fig. 2.2 and the failure load, P, is recorded. The failure load is transformed to the splitting tensile strength using the formal relation

$$f_{splitting} = \frac{2P}{\pi l d} \tag{2.1}$$

which is based on assumptions of the stiffness properties, [2] and [12].

The dogbone specimens were cast in wood moulds and stored in a lying condition for the first 18 hours at about 20 $°C$ and then the moulds were removed. The specimens were then sealed in thick alu-coated plastic bags and kept at 20 respectively 40$°C$ until the time of testing. The splitting specimens were cast in plastic moulds and stored similarly.

Development of Elastic Modulus and Strength

At the day of testing three dogbone and three splitting specimens are taken from the curing place. The dogbone specimens are glued into the steel cups and fastened in the testing machine. In the first test series only the strength development is measured and in the following the development of the modulus of elasticity is also measured. This is because the strength is needed to determine different load levels for the modulus of elasticity test. The development of the modulus of elasticity is determined by loading the specimen in tension until 45% of the tensile strength and record the deformations and the stress. The deformations are measured using clip gauges on two opposite sides and the average signal

is used in the analysis. This loading sequence is repeated 5 times and then the same procedure is followed once more to the load level 60% of the tensile strength.

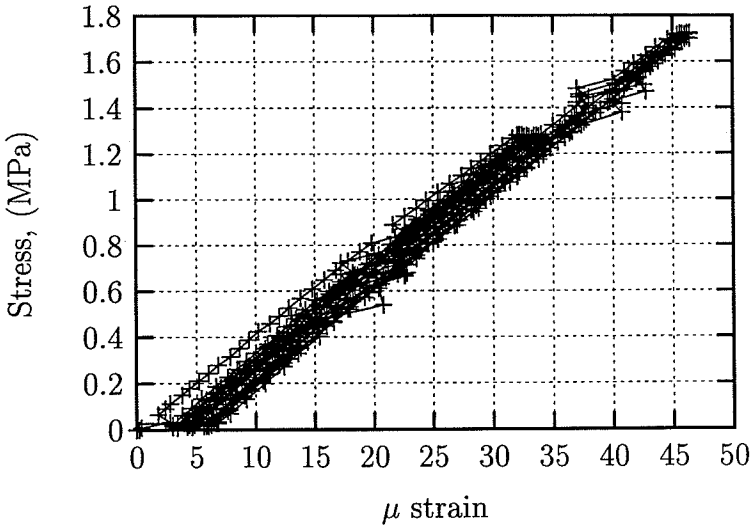

Figure 2.3: Stress-strain relationship.

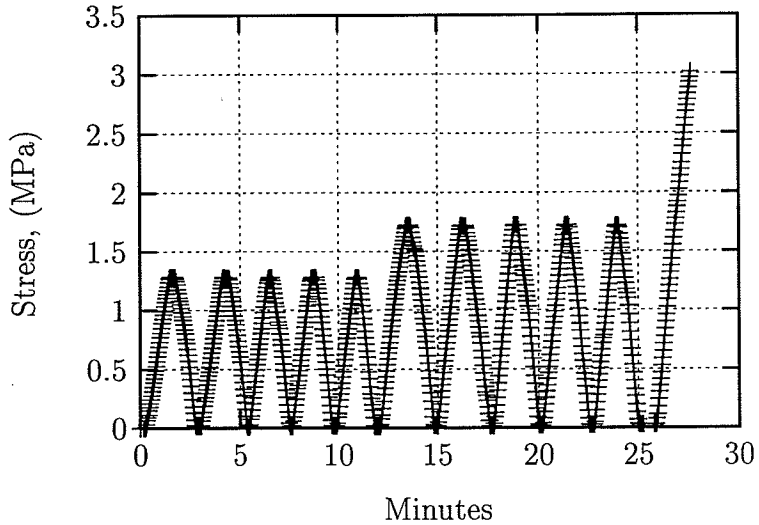

Figure 2.4: Loading history for the modulus of elasticity.

Fig. 2.3 shows an example on the stress-strain relationship obtained for the measurements of the modulus of elasticity after 168 hours of hydration at $40°C$. It is seen that the measured points are within the linear range and then the obtained development of the modulus of elasticity consists of tangential values. The loading history is seen in Fig. 2.4 and 5 cycles to the load level 45% and 60%, respectively, are shown. After the 10 cycles the specimen is loaded until failure and the recorded one-dimensional tensile strength is 3 MPa. The development of the splitting tensile strength is measured in the standard way.

2.1.2 Compression

After casting the compressive specimens are cured in the moulds for the first 18 hours and then they are kept sealed in plastic bags in a water bath at 20 and $40°C$, respectively, until the day of testing. The standard on making and curing specimens, [19], prescribe that the specimens are placed in the water baths without sealing at least after 72 hours after casting so our method differ at this point.

The compressive modulus of elasticity and strength development are measured from a loading history where the load level is gradually increased until failure as shown in Fig. 2.5 for a concrete which has hydrated for 18 hours at $20°C$. After about 30 seconds the rate of loading is increased. This loading history differ from the ones prescribed in the standards, [22] and [20], however, it is assumed that the influence is small.

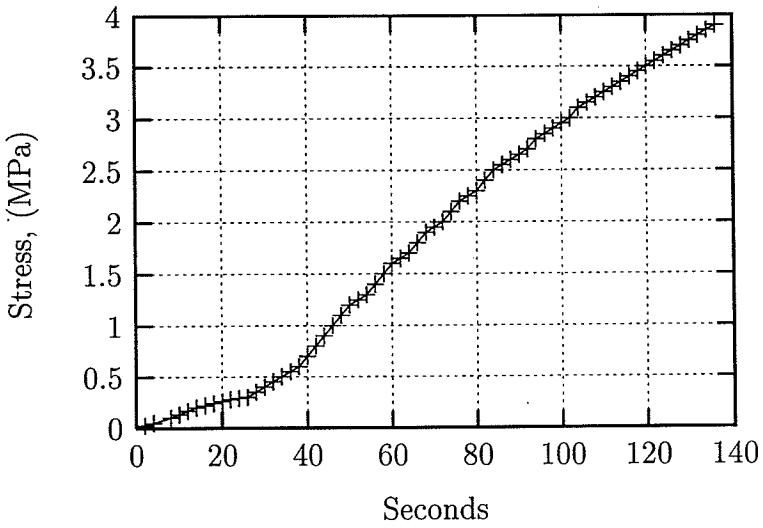

Figure 2.5: Loading history.

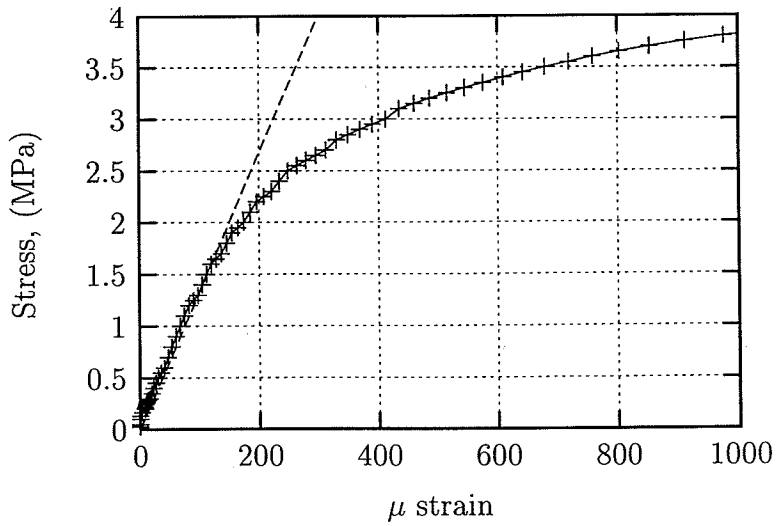

Figure 2.6: Stress-strain relationship.

Fig. 2.6 shows the stress-strain relationship obtained in the test and it is seen that the compressive strength is 3.9 MPa. Also shown is the regression line used for determining the modulus of elasticity and the points used in the regression corresponds to the ones below 20% of the strength. In this range the stress-strain relationship is linear so the measured modulus of elasticity is a tangential value.

2.2 Creep and Relaxation

2.2.1 Developed Specimen

Axi-symmetric dogbone specimens have been designed for the tensile creep experiments. The moulds are shown in Fig. 2.7 together with a specimen.

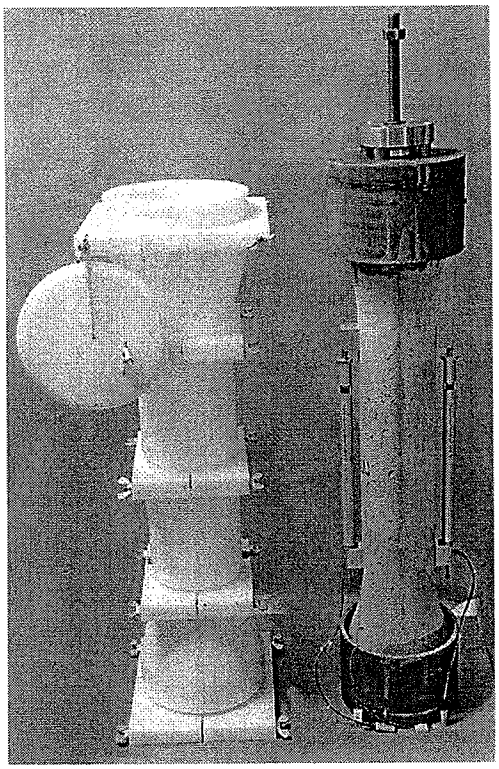

Figure 2.7: Tensile creep specimen. Teflon mould and specimen glued into steel cups.

The same principle of glueing steel cups to the specimen and applying load to the specimen as in the tensile strength experiments is used. The moulds are made of teflon and they are flexible with a cylinder shaped center and two conical shaped ends as shown. For the compressive creep and relaxation tests the same moulds are used, however, only the mid section since no reduction of the area is needed. The dimensions of the specimen shown in Fig. 2.7 are

- total length = 960 mm, length cylindersection = 480 mm
- end diameter = 190 mm, cylindersection diameter = 130 mm

The zone between the end and the cylinder section is conical shaped and the radius of curvature is 125 mm. The thick end of the specimens has a diameter of 190 mm. The steel cup has an inner diameter of 200 mm meaning that the thickness of the glue layer is 5 mm which is prescribed by the manufacturer, [8]. The LVDTs used for the strain measurements have been attached in Fig. 2.7 for illustration purpose only since the tests were carried out in a sealed condition. The connection mounts between the concrete and the heads of the LVDTs are fastened to steel pins of a diameter of 6 mm through the specimen. The measurement length is 400 mm. Stiff steel blocks are mounted to the steel pins and the LVDT is placed in between as seen in Fig. 2.7. It was found to be of importance that the connection is very stiff since an accuracy of the order of 5 μ is needed in the tensile creep experiments and in the shrinkage measurements on the dummies. To avoid rotation of the pins when fastening the steel blocks two blade nuts are screwed against each other on the pins in the middle of the specimen.

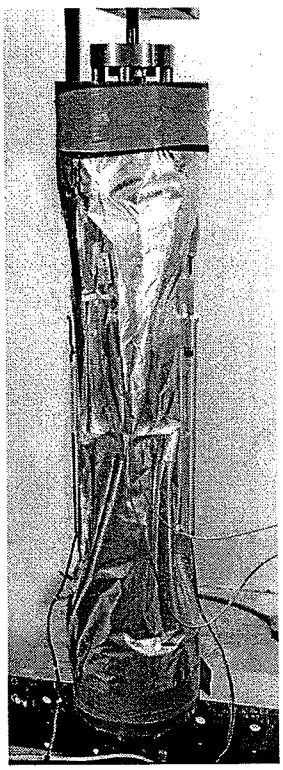

Figure 2.8: Sealing with alu-coated plastic foil.

Sealing is carried out as shown in Fig. 2.8 with welded alu-coated plastic foil bags and heavy tape. For testing whether the chosen sealing was sufficient an analysis was carried out, where different types of sealing was used for a 100 mm $\times$ 200 mm cylinder and the weight loss in time was recorded. Fig. 2.9 shows the weight loss as a function of time. Three types of sealing were tested

- thin plastic foil, thickness 12 μ, 3 layers
- thin plastic foil, thickness 12 μ, 6 layers

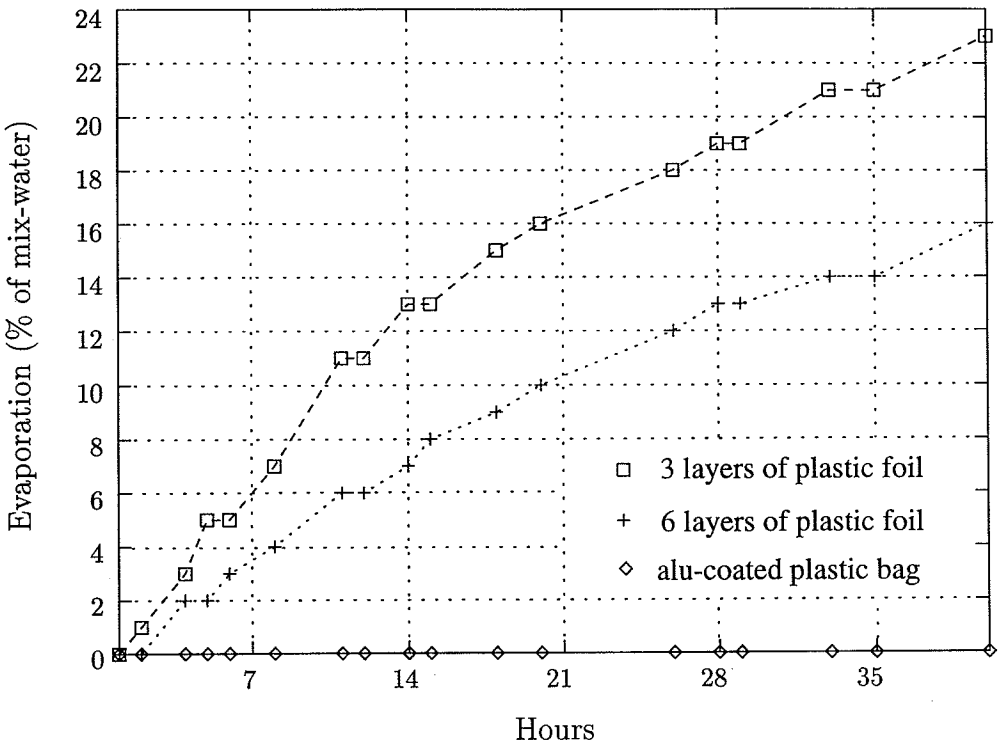

Figure 2.9: Evaporation using various sealings.

- the alu-coated plastic bags used in the present context

The plastic foil correspond to what is currently used in practice and it is seen that the weight loss measured as percentage of the mix-water increases with time up till 23% for the 3 layers sealing and up till 16% for the 6 layers sealing. In the case of the alu-coated plastic bags less than 0.1% weight loss took place within the test period extending over 40 days which exceeds the test period of interest in the present context. The water loss in the case of the plastic foil may affect the shrinkage. After casting the moulds were placed horizontally to avoid settlement cracking and minimize the differences in strength development due to gravity, [4]. The specimens are cured in the moulds during the first about 24 maturity hours. Then the steel cups are glued to the specimen and they are placed in the alu-coated plastic bags and fastened in the testing machine. During this period the dummy and the loaded specimen follows each other as far as possible.

2.2.2 Loading Rig for the $20°C$ Tests

The loading rig developed for testing of concrete in tension and compression at $20°C$ is shown in Fig. 2.10. The rig is build up using beam and column elements. It is placed in an indoor climate at an undisturbed location where the temperature is almost constant. During one test 6 specimens may be tested, two in compression and four in tension. The specimens in tension are identically loaded two by two and the two specimens in compression may be differently loaded.

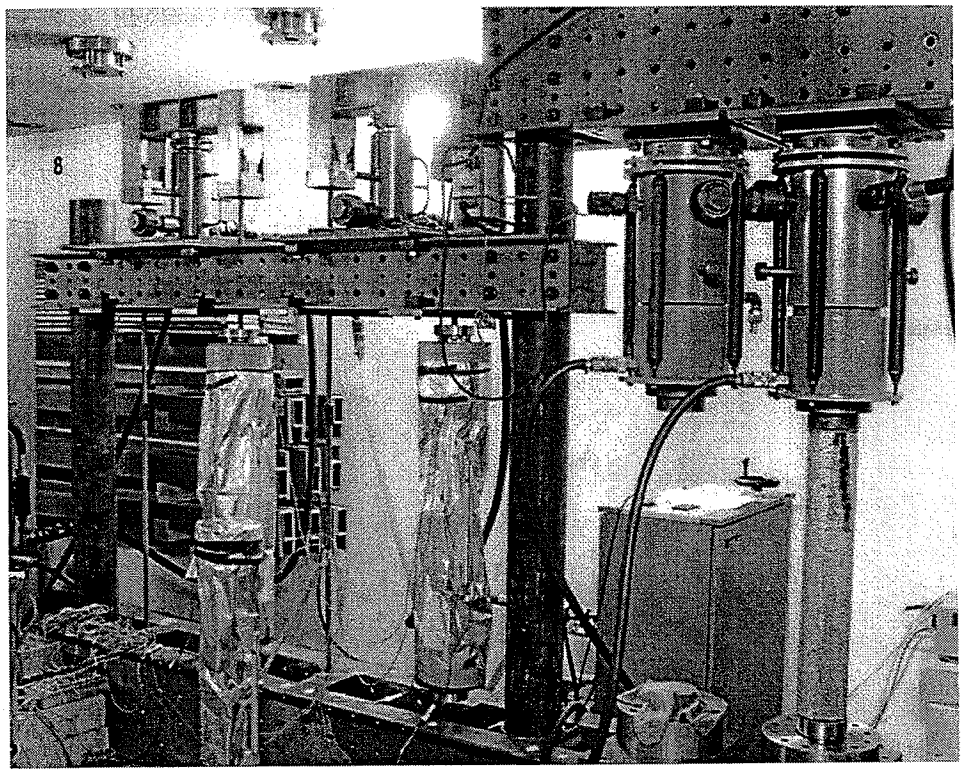

Figure 2.10: Loading rig for tension and compression.

The situation in Fig. 2.10 shows two tensile specimens which are sealed and one unsealed compressive specimen. The tensile specimens are loaded through a yoke and in Fig. 2.10 a steel bar has substituted two tensile specimens. The compressive specimen is only placed for illustration purpose. In front of the setup the dummy specimen is seen standing on the floor.

The temperature is measured in the center and near the surface of each specimen at the cross-section where the pins are located. Temperature measurements are started after casting to determine whether gradients occur.

2.2.3 Loading Rig for the 40°C Tests

A testing machine with both load and deformation control in tension and compression was developed to perform creep and relaxation tests. Fig. 2.11 shows the equipment placed in the temperature control hut. The temperature in the specimen are controlled using two electrical heaters and circulating the air with two electrical fans. The walls are 80 mm thick foam with an aluminium plate on each side. This allows for testing at a temperature history which resemble a practical situation with a period of increasing temperatures followed by a cooling period. The PC for data acquisition is placed outside the hut so that the door may be kept closed during the test.

Fig. 2.12 shows details of the specimens which are placed close to each other to have the same temperature history. The sealing is the alu-coated plastic bags. In the example

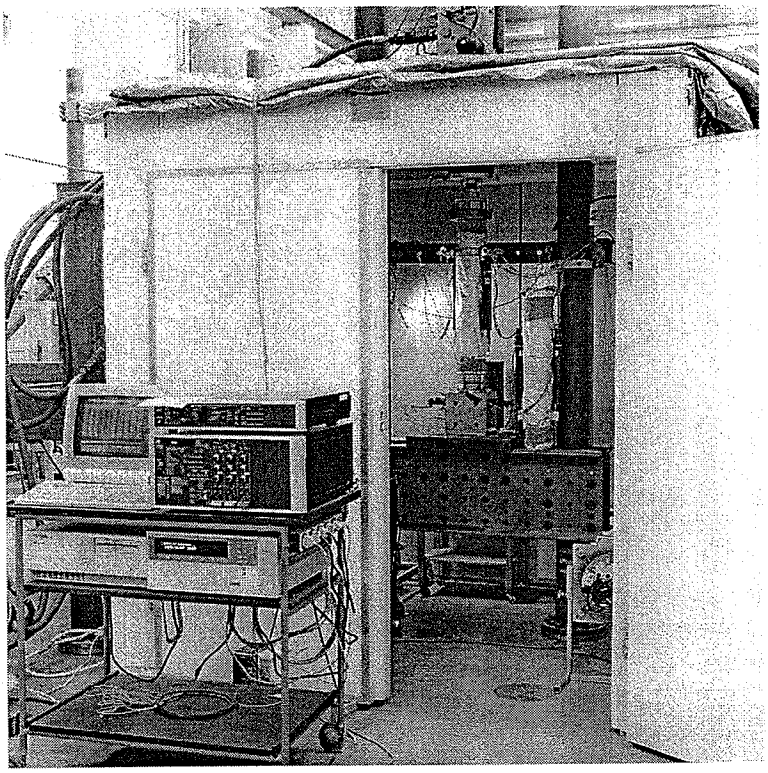

Figure 2.11: Survey of the Temperature Testing Equipment.

a compressive test is being carried out but testing of the dogbone shaped specimens are also possible. The strains are measured on each side of the specimen using graphite based transducers with LVDTs. This construction makes the LVDTs almost insensitive to temperature variations. The prescribed deformations of the loaded specimen in the relaxation experiments may follow a control signal e.g. measured on the unloaded dummy.

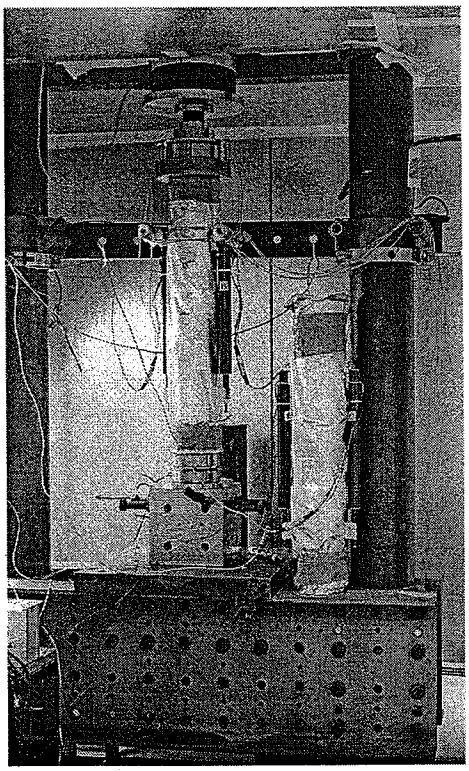

Figure 2.12: Specimen placed in the heat control hut.

Chapter 3

Results

3.1 Tensile Properties at $20°C$

3.1.1 Modulus of Elasticity and Tensile Strength

The modulus of elasticity and the tensile strength was measured at the terms about 26, 70, 170, 358 and 700 hours using the developed dogbone specimens. Appendix A.1 shows the results. One datapoint is missing at the terms 358 and 700 hours because of failure in the glue. The lower value of the modulus of elasticity correspond to the loading sequence from zero load till 45% of the tensile strength and the upper value correspond to 60% of the tensile strength. Fig. 3.1 shows the elastic modulus plotted as a function of time.

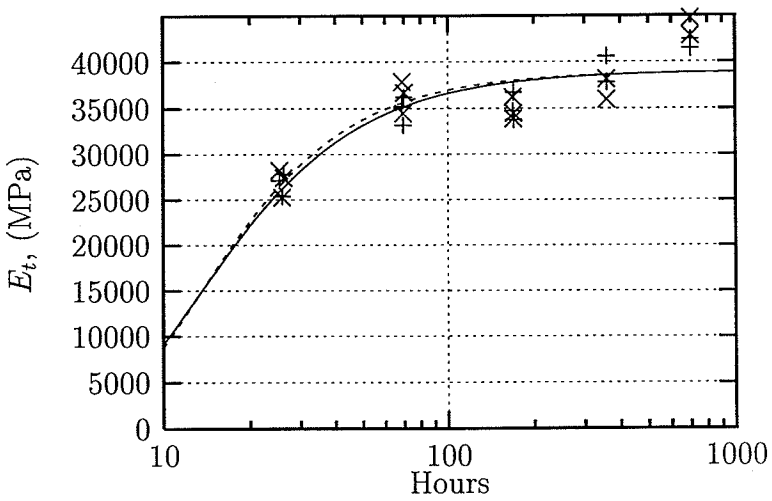

Figure 3.1: Development of the modulus of elasticity at $20°C$.

Also shown is the best fit obtained with a function of the form

$$E(t) = E^{\infty} \exp(-(\frac{\tau}{t})^{\alpha}) \tag{3.1}$$

which normally is used for numerical purposes, [5]. The optimal parameters were calculated as

- lower: $E^{\infty} = 39.0$ GPa, $\tau = 13.17$ hours and $\alpha = 1.36$
- upper: $E^{\infty} = 38.9$ GPa, $\tau = 13.16$ hours and $\alpha = 1.46$

Fig. 3.1 shows that the upper and lower value of the modulus of elasticity are almost identical. The splitting tensile strength has been measured at the terms 20, 46, 71, 168, 336 and 672 hours. Appendix A.2 shows the results. The optimal parameters were calculated as

- one-dimensional: $f^{\infty} = 2.9$ MPa, $\tau = 26.17$ hours and $\alpha = 1.4$
- splitting: $f^{\infty} = 4.8$ MPa, $\tau = 61.4$ hours and $\alpha = 0.44$

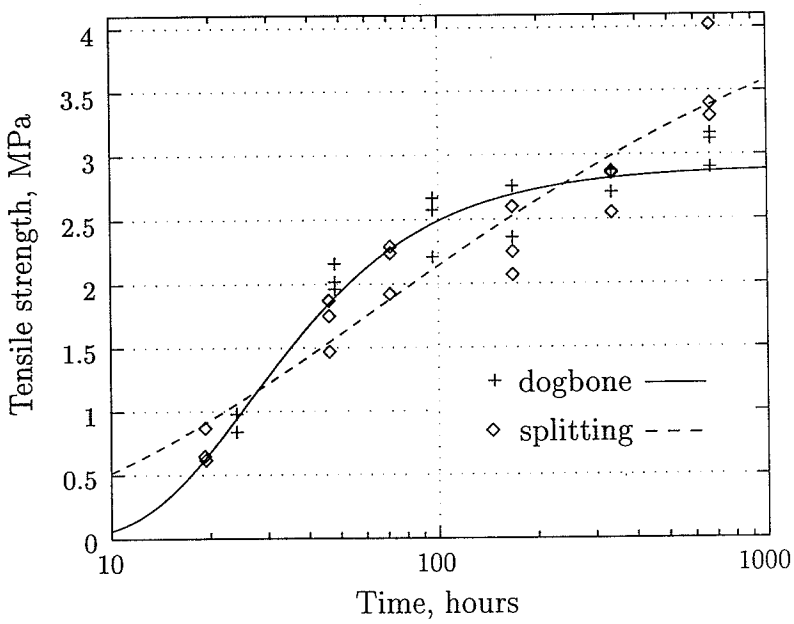

Figure 3.2: One-dimensional and splitting tensile strength, $20°C$.

Fig. 3.2 shows the tensile strength values plotted together with the optimal fit.

3.2 Tensile Properties at $40°C$

3.2.1 Modulus of Elasticity and Tensile Strength

The modulus of elasticity and the tensile strength was measured at the terms 25, 45, 50, 72, 169, 338 and 698 hours using the developed dogbone specimens and Appendix A.3 shows the results. The datapoint missing at the term 338 hours is because of failure in the glue. Fig. 3.3 shows the modulus of elasticity plotted as a function of time.

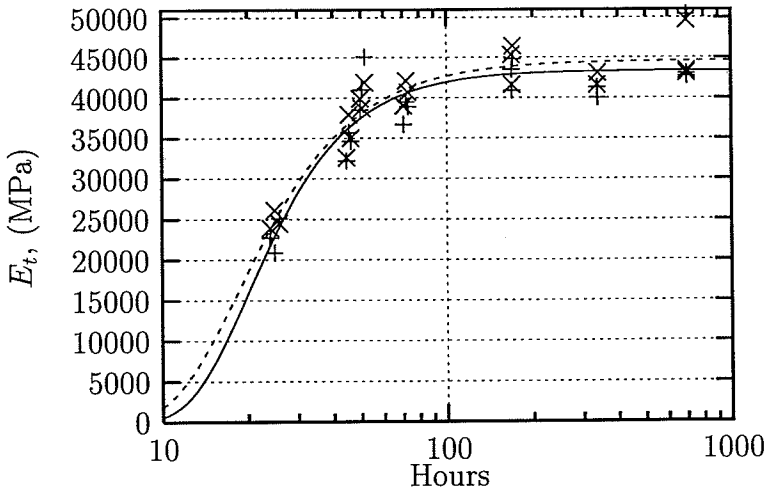

Figure 3.3: Development of the modulus of elasticity at $40°C$.

Also shown is the best fit obtained with the exponential type function and the optimal parameters were found to

- lower: $E^{\infty} = 43.4$ GPa, $\tau = 20.08$ hours and $\alpha = 2.11$
- upper: $E^{\infty} = 44.6$ GPa, $\tau = 18.67$ hours and $\alpha = 1.86$

Fig. 3.3 shows that the upper and lower value of the modulus of elasticity are almost identical. The splitting tensile strength has also been measured at $40°C$ and Appendix A.4 shows the results. The last set of datapoints shown in Appendix A.4 has been measured from another batch cast later than the first ones and this may explain why they are remarkably larger. The optimal parameters were found to

- one-dimensional: $f^{\infty} = 6.3$ MPa, $\tau = 56.72$ hours and $\alpha = 0.34$
- splitting: $f^{\infty} = 4.5$ MPa, $\tau = 37.24$ hours and $\alpha = 0.78$

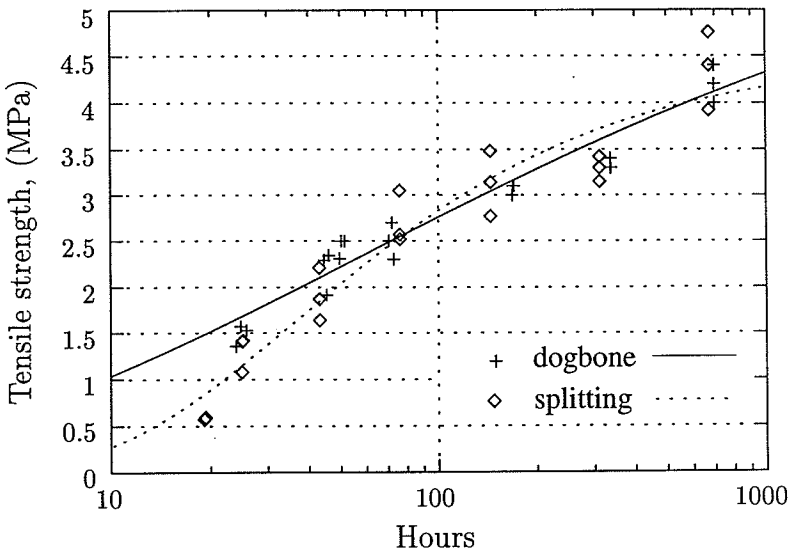

Figure 3.4: One-dimensional and splitting tensile strength, $40°C$.

Fig. 3.2 shows the tensile strength values plotted together with the optimal fit. The tensile strength results measured at $40°C$ are dubious due to problems in testing and casting.

3.3 Tensile Properties, Discussion

3.3.1 Modulus of Elasticity

The development of the modulus of elasticity in tension at the two temperature levels have been compared in Fig. 3.5 using maturity hours on the abscissa. Based on the results it can not be concluded that the maturity concept does not work properly for a description of the development of the modulus of elasticity.

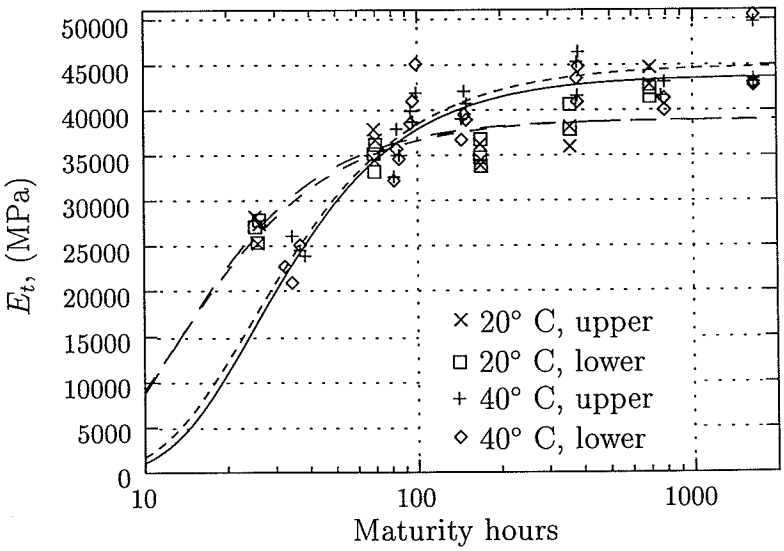

Figure 3.5: Modulus of elasticity in tension, at 20 and $40°C$.

3.3.2 Tensile Strength

From the optimal fits at $20°C$ shown in Fig. 3.2 it becomes apparent that the one-dimensional strength exceeds the splitting strength earlier than about 2 weeks whereas the opposite holds true at later ages. Due to the problems in the tensile strength measurements at $40°C$ the present discussion focus on the results shown in Fig. 3.2. According to [10] the one-dimensional tensile strength is obtained from the splitting strength using a reduction factor of 0.6. However, this seems to be the case only for old concrete as seen from Fig. 3.2 where the ultimate one-dimensional strength is 0.6 times the ultimate splitting strength.

At early age the Poisson's ratio is 0.5 immediately after start of hydration where the concrete behaves as a liquid. In the following hours, the setting time, the Poisson's ratio decrease to a minimum followed by an increase until a final value of about 0.2, e.g. [4] and [16], and Fig. 3.6 shows this principal development.

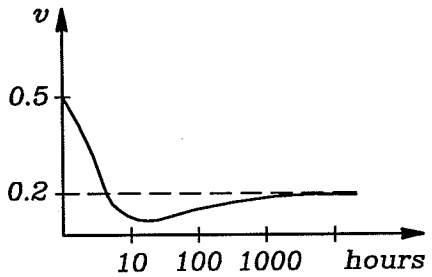

Figure 3.6: Typical development of the Poisson's ratio.

Finite element analysis of the dog-bone and the splitting experiments have been carried out to clarify if the development of the Poisson's ratio may explain the observed relation between the one-dimensional strength and the splitting tensile strength. The program used is the commercial package COSMOS, [6], and a simple crack criteria has been applied where failure takes place when the maximum principal stress reaches the tensile strength. The analysis is linear elastic and a more refined analysis could include a crack model e.g. using the smeared-out concept, [7].

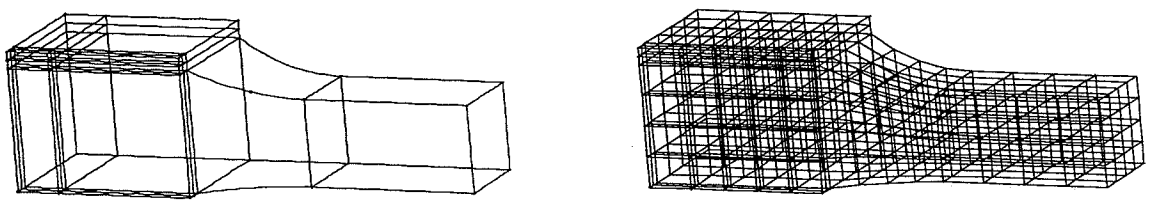

Figure 3.7: Volumes and coarsest mesh used for the dogbone analysis.

The elements are simple 3D SOLID´s with 8 nodes, [6], and Fig. 3.7 shows the volumes and the coarsest mesh used in the analysis of the dogbone test. Due to symmetry only 1/8

of the specimen is modelled. The load is applied on the thick steel plates at the ends. The concrete, glue and steeel volumes are also seen in Fig. 3.7.

The volumes and the coarsest mesh used for the modelling of the splitting test are seen in Fig. 3.8 and the volumes are concrete, wood and steel volumes respectively.

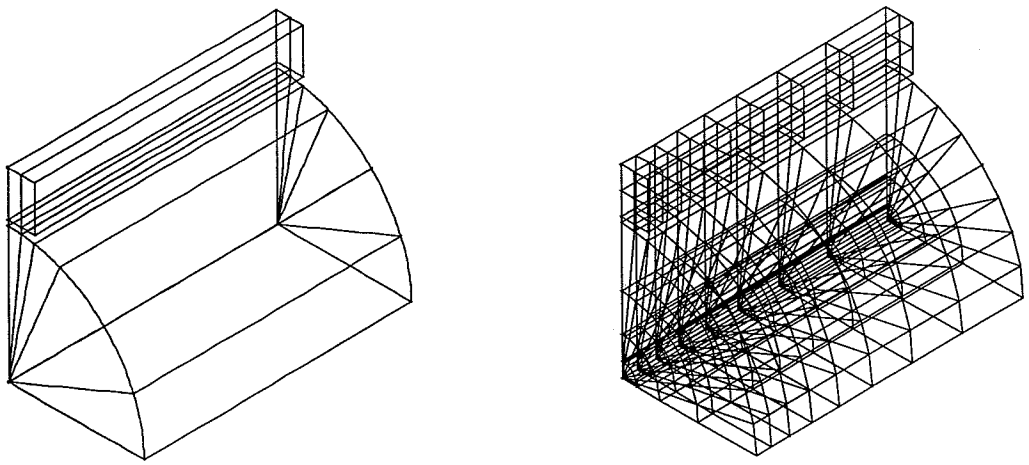

Figure 3.8: Volumes and coarsest mesh used in the splitting test.

The material properties chosen for the analysis are 4 different values of the Poisson's ratio, $\nu = 0.1$, 0.2, 0.3 and 0.4, respectively, and the constant elastic moduli $E_{concrete} = 2.0\ 10^4$ MPa, $E_{glue} = 2.3\ 10^4$ MPa, $E_{steel} = 21.0\ 10^4$ MPa and $E_{wood} = 2.0\ 10^3$ MPa. The elastic moduli are chosen as typical values for concrete, steel and wood and the value for the glue are provided by the manufacturer, [8]. The tensile strength has been chosen to $f_t = 1.0$ MPa.

Initially, a convergence study was carried out where the meshes were refined until the change in the maximum principal stress became less than 5 %. The result is shown in Table 3.1 and mesh *a* correspond to the element level shown in Fig. 3.7 and Fig. 3.8 with 303 elements in the dogbone case and 296 elements in the splitting case. Mesh *b* is obtained from mesh *a* by halving each element side and mesh *c* is obtained from mesh *b* in a similar way.

Mesh	Splitting	Dogbone
a	6.98	2.45
b	7.43	2.71
c	7.74	2.75

Table 3.1: Result of convergence study.

From Table 3.1 it is concluded that an acceptable accuracy has been obtained with mesh *c* and this mesh has been used in the following. Fig. 3.9 shows the value of the one-dimensional and splitting tensile strength, respectively, giving a maximum principle tensile

stress equal to the tensile strength, $f_t = 1.0$ MPa, and thus failure, as a function of the Poisson's ratio.

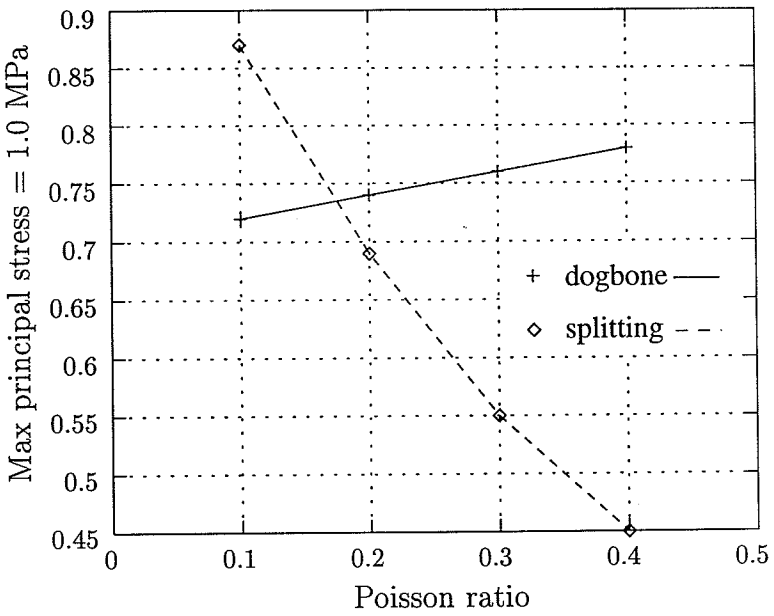

Figure 3.9: Value of the two strengths giving failure.

As an example take the calculated strength values for a Poisson's ratio of 0.3 from Fig. 3.9 which are $f_{dogbone} = 0.76$ MPa and $f_{splitting} = 0.55$ MPa, respectively. These values show that for an average stress of 0.76 MPa in the dogbone test failure occur whereas a splitting strength value of 0.55 MPa, calculated according to (2.1), gives failure. It is seen that the influence of the Poisson's ratio on the strength value giving failure is largest in the case of the splitting strength and a change with a factor 4 of the Poisson's ratio changes the strength with almost a factor 2. For the one-dimensional case the corresponding change is only about 5 %. Further a shift in behavior is observed and at very early age, when the Poisson's ratio is relatively large, the one-dimensional strength exceeds the splitting strength whereas the opposite is the case later. This confirms the tendency observed in the experiments shown in Fig. 3.2. It is assumed that including a more refined crack model would not change the general result shown in Fig. 3.9 but cause a translation of the two curves corresponding to the residual capacity. This translation is probably largest in the splitting test because stress redistributions have larger influence here.

3.4 Tensile Properties, Creep at $20°C$

3.4.1 Age at Loading 24 hours

Fig. 3.10 shows the loading histories obtained in the tensile creep tests. Each test includes two loaded specimens and the variation between the load on each specimen is less than 5%.

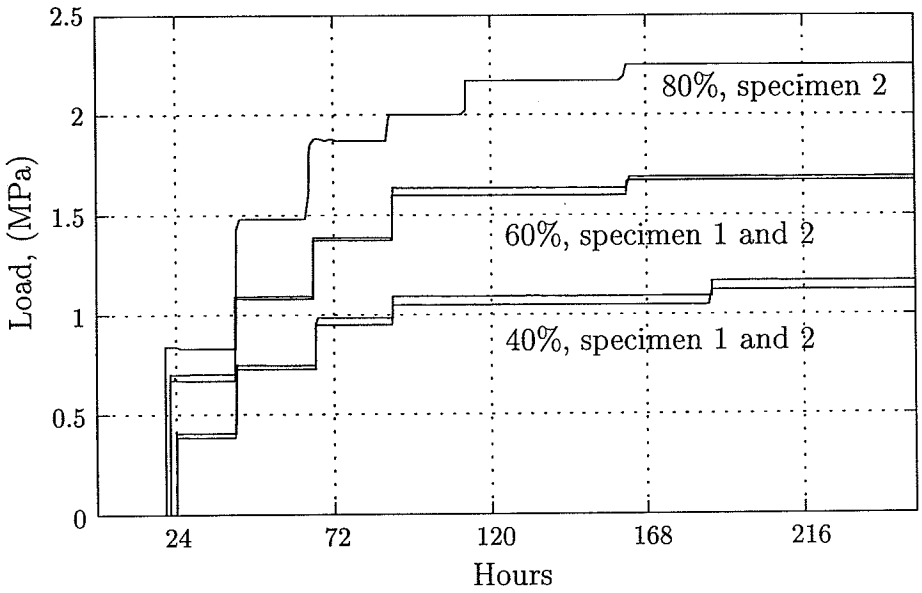

Figure 3.10: Load history in the tests. Age at loading 24 hours.

Fig. 3.11 shows the load expressed as a percentage of the current tensile strength. The tensile strength development used was the one-dimensional obtained from the dogbone tests shown in 3.2. The decrease is due to the progress of hydration. The wanted load levels in the tests are 40, 60 and 80% respectively. This is fulfilled mainly in the late terms where hydration has almost ceased.

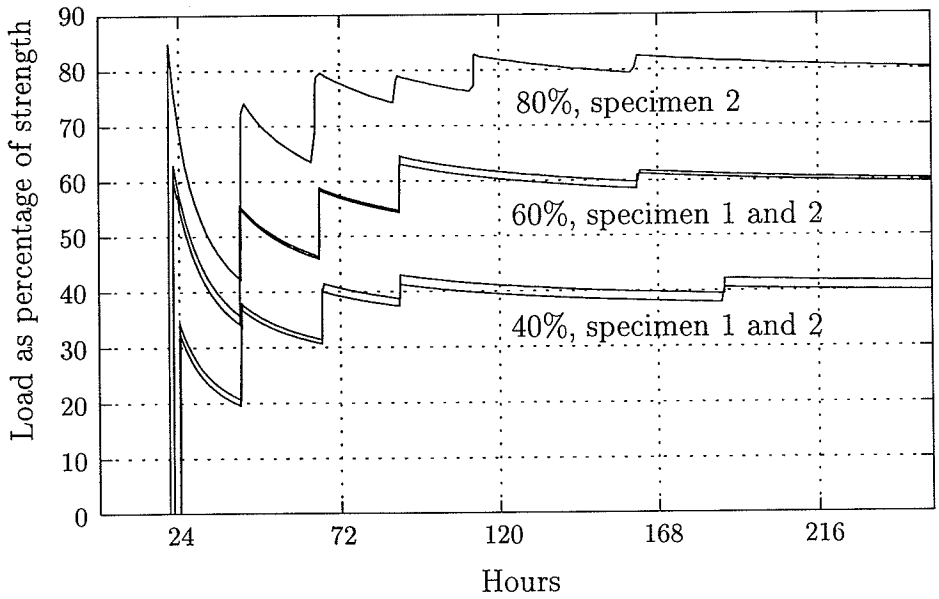

Figure 3.11: Relative load history in the tests. Age at loading 24 hours.

Fig. 3.12 gives a summery of the measured creep. The complete curves are repeated in Appendix C.1 together with the measured shrinkage and temperature development. The curves show the load induced strains which is the raw data compensated for shrinkage and

thermal deformations. The temperature was measured in both the loaded specimen and the dummies and the maximum difference in temperature was about $3°C$. The difference was largest after form removal and this indicate that the thermocouples were placed too close to the surfaces of the specimens. Therefore the temperature development after form removal used in the thermal compensation is obtained from an extrapolation of the later temperature development to the temperature before demoulding. The coefficient of thermal expansion used in this compensation was 9.0 μ strain/$°C$. After compensation the results are consistent and the temperature compensated shrinkage of all the tests have a maximum value of about 35-50μ strain which is close to the shrinkage measured on the concrete and reported in [11].

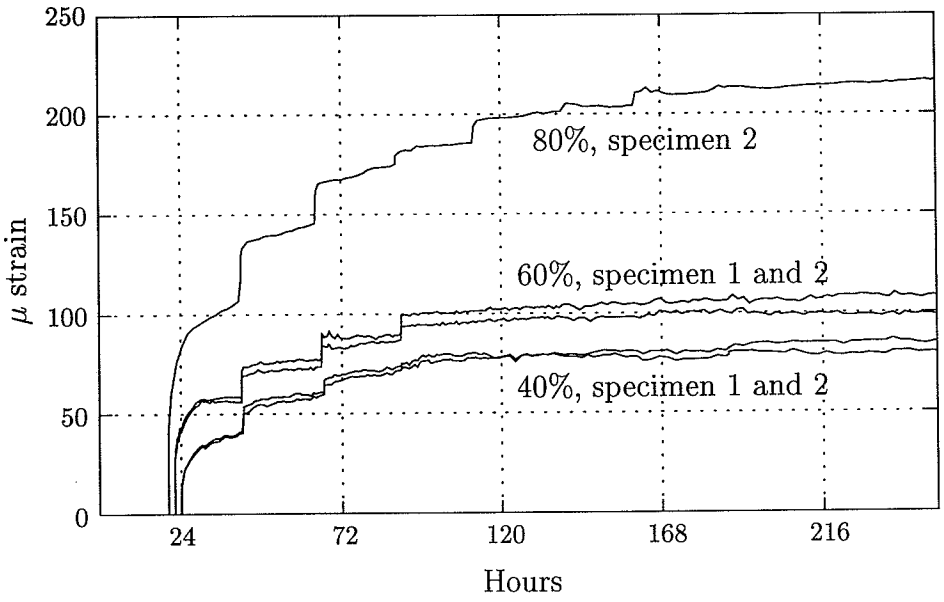

Figure 3.12: Measured creep in tension. Age at loading 24 hours.

The second specimen at the load level 80% failed after application of load and thus only one curve in Fig. 3.12 is available here. Each curve in Fig. 3.12 is an average of the measurements on each side of the specimen and the difference between the two loaded specimen at 40% and 60% load level respectively is rather little.

3.4.2 Age at Loading 72 hours

Fig. 3.13 shows the loading histories obtained in the creep tests loaded after 72 hours of hydration and Fig. 3.14 shows the relative load level. Since the increase in tensile strength is low from 72 hours and onwards the variation in relative load level is also low which means that the obtained load levels are close to the wanted ones.

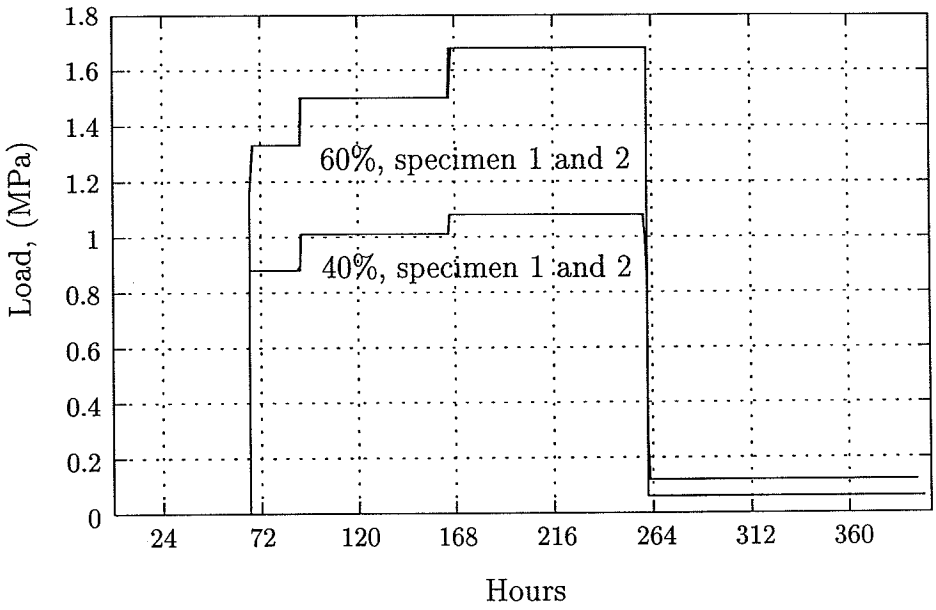

Figure 3.13: Load history in the tests. Age at loading 72 hours.

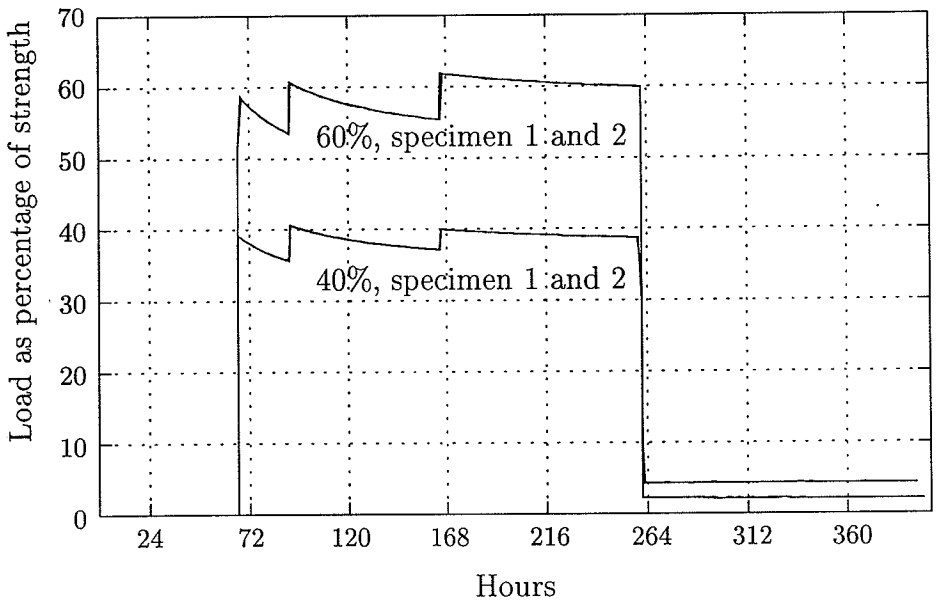

Figure 3.14: Relative load history in the tests. Age at loading 72 hours.

Fig. 3.15 shows the measured creep and each curve is the average of measurements on each side. Appendix C.2 shows the individual load levels together with the measured shrinkage and temperature development.

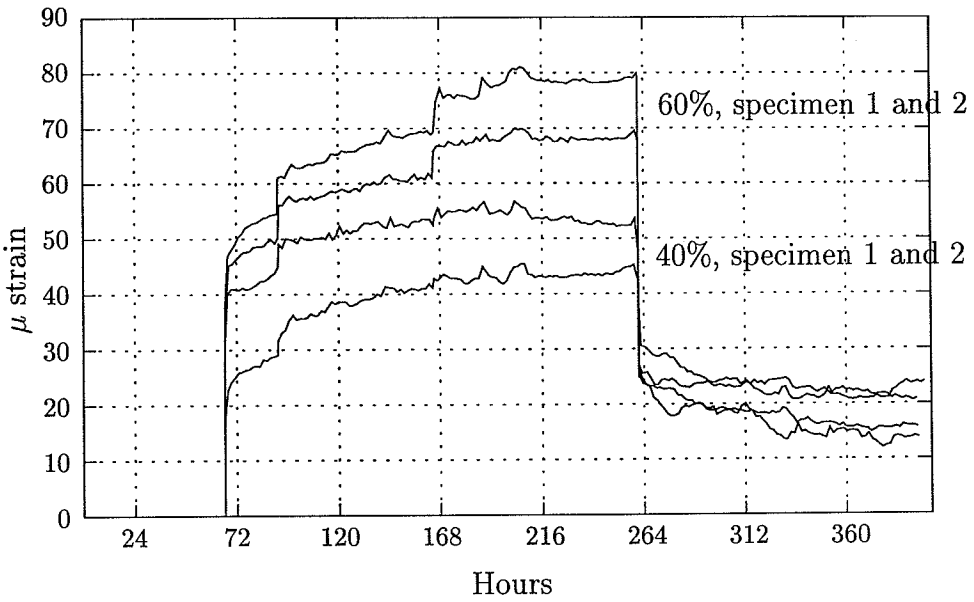

Figure 3.15: Measured creep in tension. Age at loading 72 hours.

3.4.3 Discussion

The creep experiments for tension, Fig. 3.12, indicate that the magnitude of creep in tension is comparable to the creep in compression reported for the same concrete in [17]. Further it seems as there are no non-linearity below 60% load level. However the non-linearity observed at the load level 80% is significant. After 250 hours the maximum average value of creep at the load levels are

- 40%: 82.2 μ strain
- 60%: 103.1 μ strain
- 80%: 216.6 μ strain

This gives the ratios $216.6/82.2 = 2.6$ and $103.1/82.2 = 1.3$, respectively, which shows that the creep at 80% load level is more than two times the creep at 40% load level. A ratio of two would be predicted by linearity. For the 60% load level the observed ratio is a little less than 1.5 which would be predicted by linearity. These linearity values are only rough estimates since the actual creep response is an integral value of the development of the properties and the loading history.

Comparing Fig. 3.12 and 3.15 the influence from the age at loading is seen. The ultimate value of creep for a concrete loaded after 24 hours is about 105μ strain whereas the same value for the concrete loaded after 72 hours is about 75μ strain. Each curve is the average of measurements from two sides of the specimen and the difference is up to about 30%. This is a normal level of skewness when making creep measurements on concrete.

3.5 Compressive Properties at $20°C$

3.5.1 Modulus of Elasticity and Compressive Strength

The measured development of modulus of elasticity and compressive strength at $20°C$ is shown in Appendix B.1. The values were measured at the terms 18, 48, 72, 168, 336 and 672 hours using three specimens. Fig. 3.16 and 3.17 shows the results and the optimal fit with the function of type (3.1). The optimal parameters are

- modulus of elasticity: $E^{\infty} = 38.7$ GPa, $\tau = 20.03$ hours and $\alpha = 0.97$
- compressive strength: $f^{\infty} = 35.0$ MPa, $\tau = 34.61$ hours and $\alpha = 1.06$

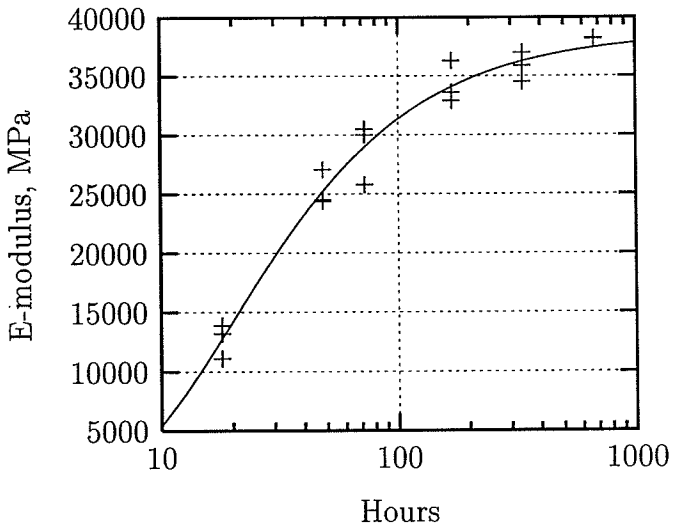

Figure 3.16: Modulus of elasticity at $20°C$.

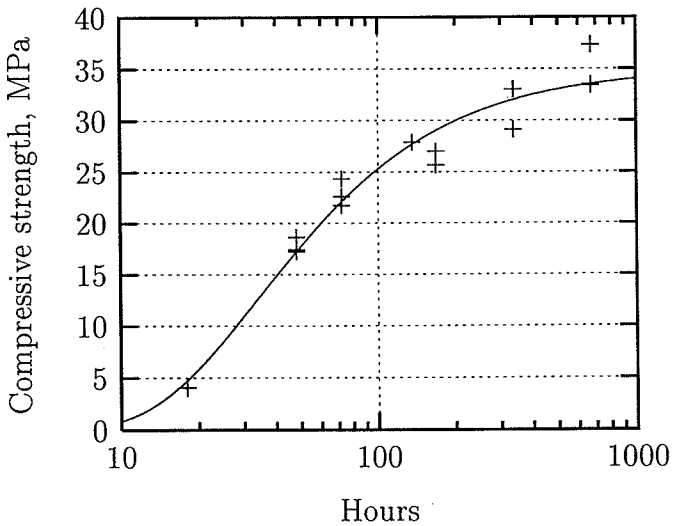

Figure 3.17: Compressive strength at $20°C$.

3.6 Compressive Properties at $40°C$

3.6.1 Modulus of Elasticity and Compressive Strength

The measured development of modulus of elasticity and compressive strength at $40°C$ is shown in Appendix B.2. The values were measured at the terms 18, 30.5, 40.5, 80.5, 150.5 and 290.5 hours using three specimens. The terms chosen correspond to approximately the same maturity as the ages in the $20°C$ case shown above. Fig. 3.18 and 3.19 shows the results and the optimal fit with the function of type (3.1). The optimal parameters are

- modulus of elasticity: $E^{\infty} = 37.2$ GPa, $\tau = 17.33$ hours and $\alpha = 1.98$
- compressive strength: $f^{\infty} = 42.4$ MPa, $\tau = 30.39$ hours and $\alpha = 1.17$

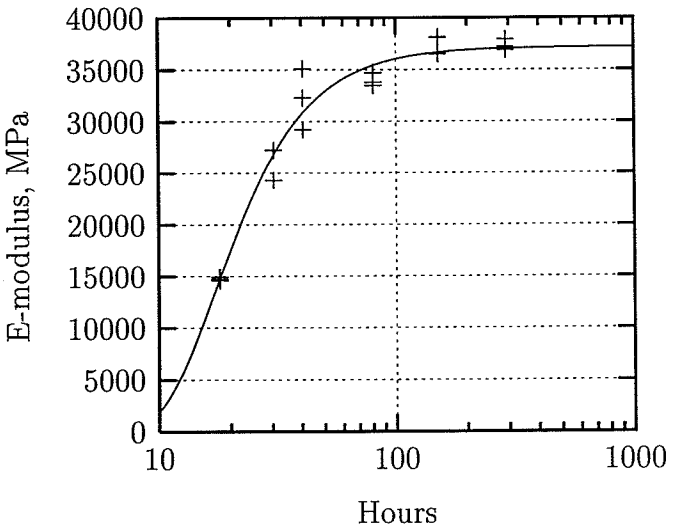

Figure 3.18: Modulus of elasticity at $40°C$.

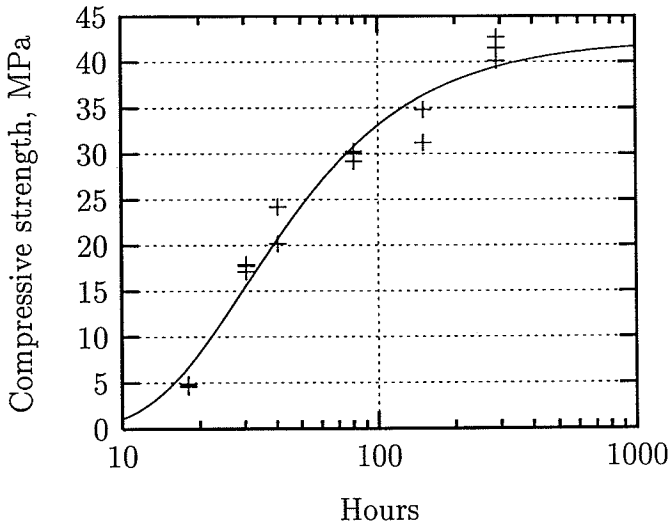

Figure 3.19: Compressive strength at $40°C$.

3.7 Compressive Properties, Discussion

3.7.1 Modulus of Elasticity

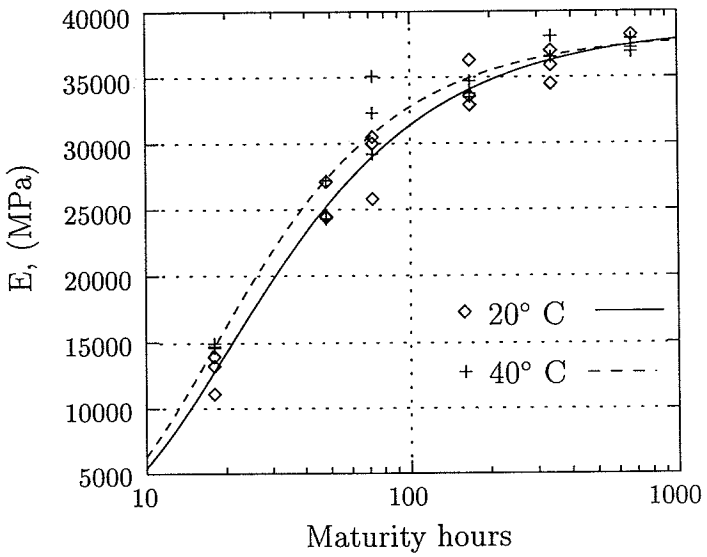

Figure 3.20: Modulus of elasticity in compression at 20 and $40°C$.

The development of the modulus of elasticity measured at the two temperature levels have been compared in Fig. 3.20 using maturity hours as abscissa. It is seen that the maturity transformation applies well to the characterisation of the results.

3.7.2 Compressive Strength

The comparison of the development of the compressive strengths is shown in Fig.3.21 and here the final value at $40°C$ exceeds the final value at $20°C$. For the first about 200 maturity hours the transformation applies well.

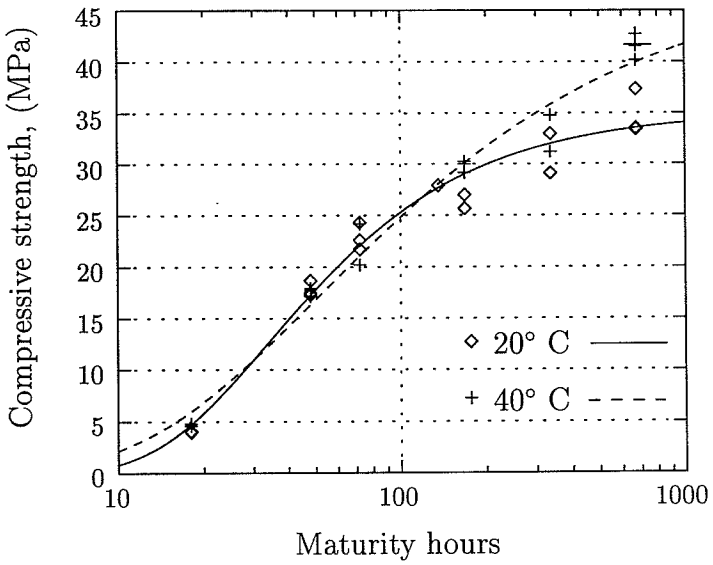

Figure 3.21: Compressive strength at 20 and $40°C$.

3.8 Compressive Creep, Age at Loading 24 hours

Creep in compression has been measured at three different temperature histories which are

- constant wanted temperature $20°C$
- constant wanted temperature $40°C$
- a variable temperature history, 20-40-$20°C$

The results are summarised in the section and the full measured developments are shown in Appendix D.1. The ages at loading were 18.5, 9.5 and 16 hours after casting, respectively, and this corresponds to almost the same maturity given the above temperature histories. The meaning of the variable temperature history is to simulate a real temperature history from practice. The load level in all three cases at first loading is about 40% of the strength and in the constant temperature cases the load is increased every 24 maturity hours as shown in Fig. 3.22.

3.8.1 Loading History

The measured loading history is seen in Fig. 3.22. In order to reduce the number of variables in the tests and isolate the effects the load is kept constant in the variable temperature case.

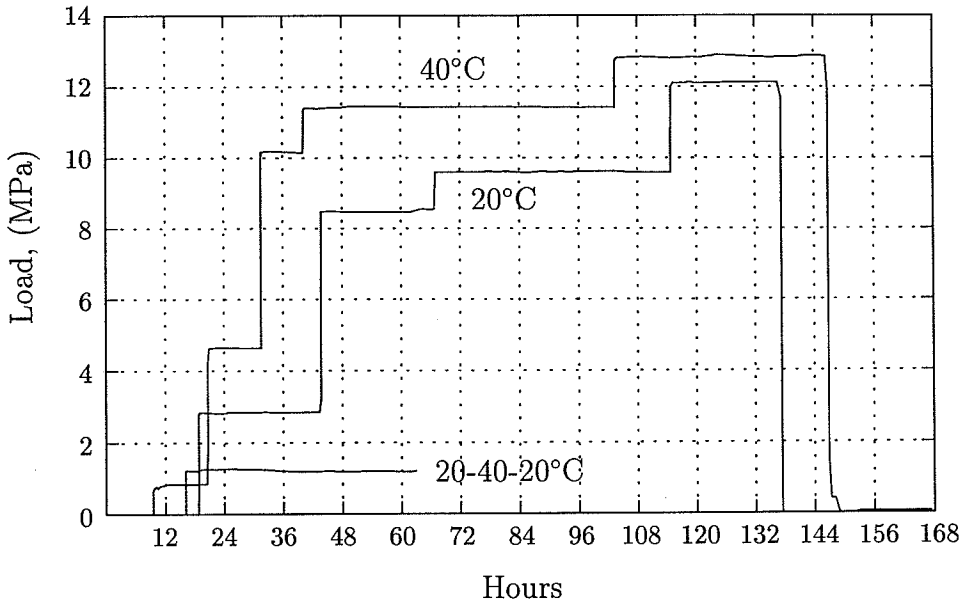

Figure 3.22: Measured loading history.

3.8.2 Temperature History

The measured temperature history is seen in Fig. 3.23. It is seen that the anticipated temperature history in the $20°C$ test was somewhat higher than $20°C$ and the $40°C$ history has a peak initially due to the hydration heat. However, the temperatures are kept constant for the rest of the tests and therefore it is concluded that the temperature control worked satisfactorily.

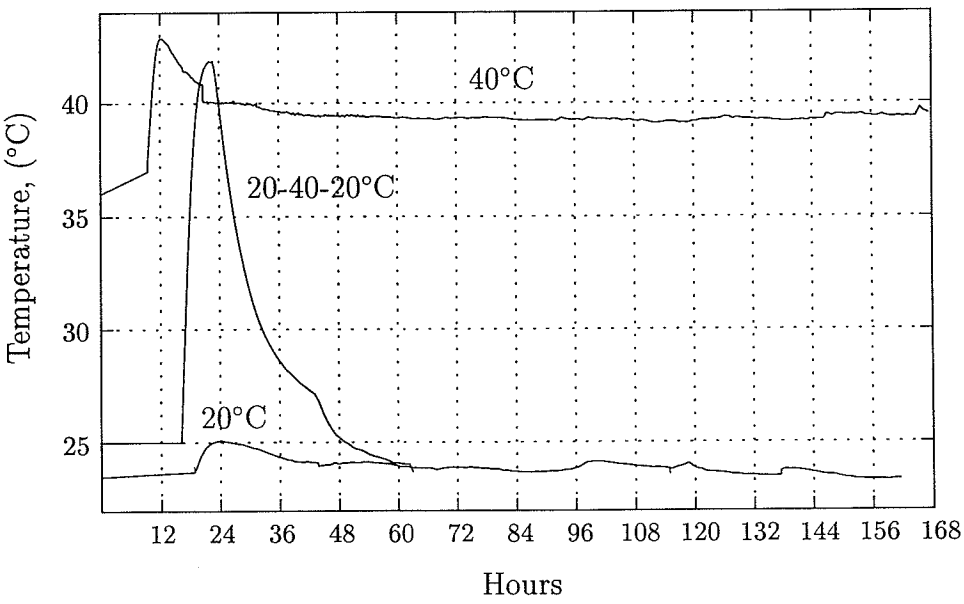

Figure 3.23: Measured temperature history.

3.8.3 Creep

The measured creep is seen in Fig. 3.24. The instantaneous deformations of the tests at $20°C$ and at the 20-40-$20°C$ history are close even though the applied stress levels are different as shown in Fig. 3.22. This is due to the maturity of the specimens at application of first load, shown in Table 3.2.

	$20°C$	$40°C$	20-40-$20°C$
t (Hours)	18.8	9.5	16.1
M (Hours at $20°C$)	22.2	19.0	17.6

Table 3.2: Time and maturity at application of first load.

Table 3.2 shows that the maturity age in the 20-40-$20°C$ test at application of the first load is less than in the $20°C$ test. However, comparing the further results at $20°C$ with the ones at the 20-40-$20°C$ history it appears that the variable temperature has a significant influence on the magnitude of creep. Even though the load remains low in the 20-40-$20°C$ test the deformations exceed the ones in the $20°C$ test. The maturity ages in the two tests are equal already 18.7 hours after mixing and from this point the maturity in the 20-40-$20°C$ test exceeds the maturity of the $20°C$ test. Further the creep at the $40°C$ test seems to exceed the $20°C$ test even though the maturity age of the two tests are about the same. However it is difficult to conclude much about the influence from a constant temperature level.

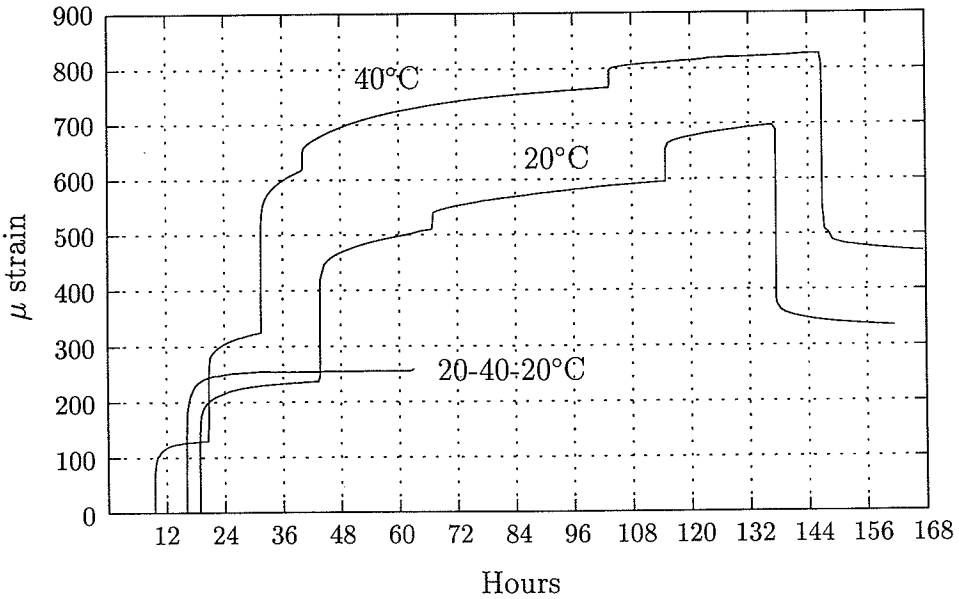

Figure 3.24: Measured creep.

Each curve shown in Fig. 3.24 represents the average of measurements from two sides of the specimen. It turned out that the difference in response from the two sides could be

large, up to 75%. However, this difference does not change the conclusions. The reason for this skewness may be due to gravity effects when the specimens are hydrating in a lying condition.

3.9 Compressive Relaxation, Age at Loading 24 hours

The relaxation properties in compression were measured and Fig. 3.25 shows the strain history. The specimen was strained after 72 hours of hydration at $20°C$ to a level corresponding to 40% of the strength. The deformations of an unloaded dummy specimen was also recorded and these measurements were used to compensate the deformations on the loaded specimen for shrinkage and thermal deformations. Thus the strain of the loaded specimens was gradually decreased during the test to compensate for the strain which was not due to mechanical load. The specimen was subjected to this strain history for almost 168 hours and then the test was stopped. The temperature difference between the loaded and the unloaded specimen was less than $0.75°C$ during the test.

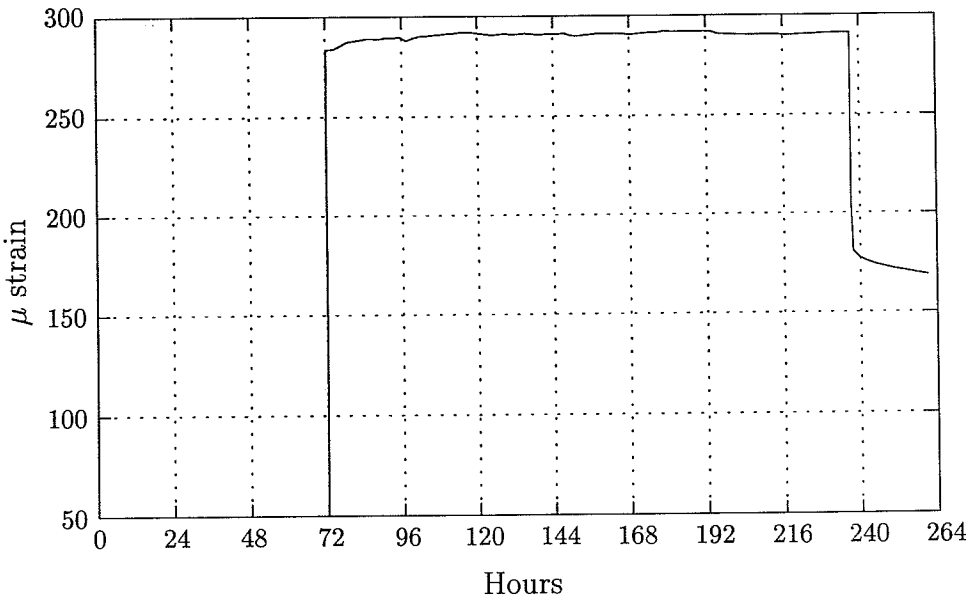

Figure 3.25: Strain history in relaxation.

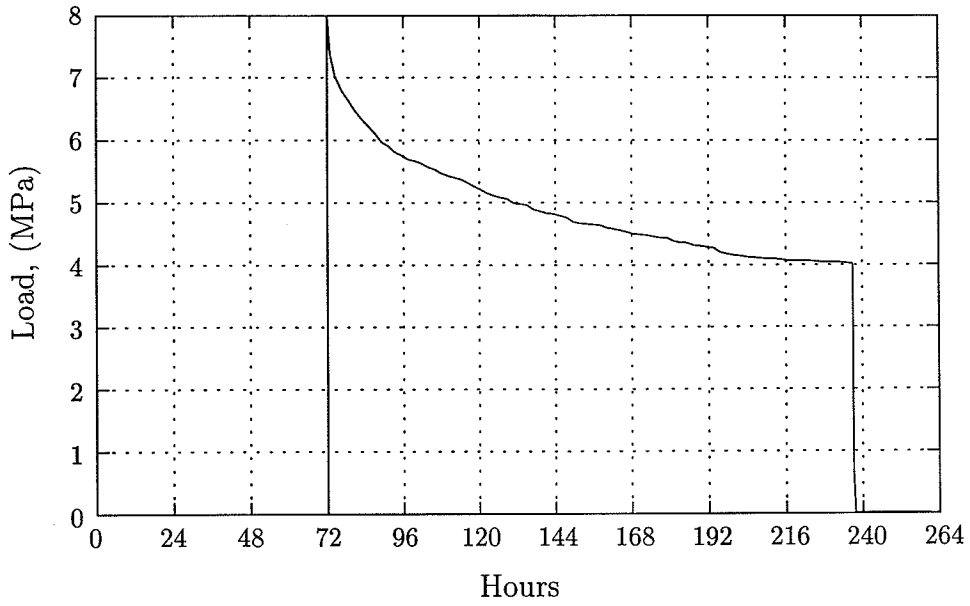

Figure 3.26: Relaxation of stresses.

Fig. 3.26 shows the stress relaxation. It is seen that the initial load level was 8.0 MPa. The stress relaxation is fast in the beginning and the rate of the decrease becomes slower with time. At the end of the experiment the stress has relaxed to 50% of the initial value and the further relaxation is seen to be small.

3.10 Comparison of Modulus of Elasticity in Tension and Compression

A comparison of the development of the moduli of elasticity in tension and compression has been carried out. The results are shown for $20°C$ in Fig. 3.27 and for $40°C$ in Fig. 3.28. Only the best fit curves are shown and the data points have been shown previously in Fig. 3.1, 3.3, 3.16 and 3.18. Based on this comparison we can not conclude that there is any difference between the modulus of elasticity in tension and in compression.

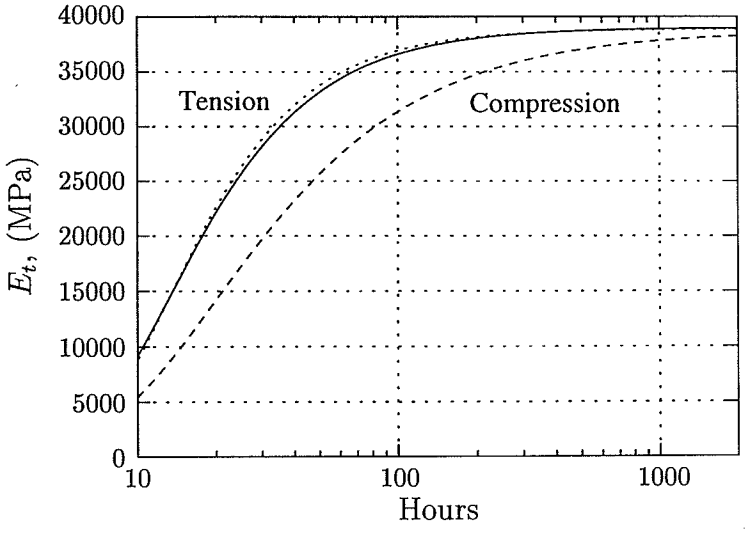

Figure 3.27: Moduli of elasticity in tension and compression, $20°C$.

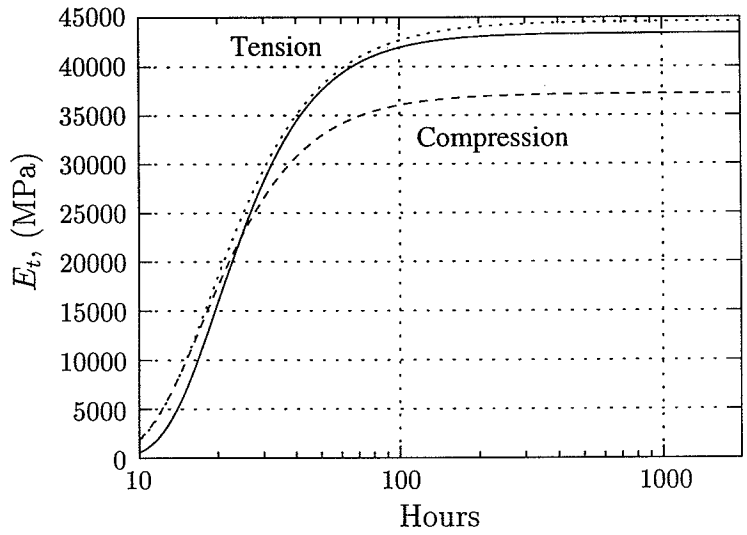

Figure 3.28: Moduli of elasticity in tension and compression, $40°C$.

Chapter 4

Conclusion

The purpose of this report was to increase the knowledge about the properties of early age concrete, particularly, in relation to

- the development of the modulus of elasticity in tension and compression
- the development of the tensile strength
- the application of the maturity concept to characterise the development of the modulus of elasticity and strength
- the creep properties in tension and compression
- non-linear creep in tension at high stress levels
- the influence of temperature levels and gradients in time
- relaxation

Experimental equipment has been developed to measure the modulus of elasticity in tension and the one-dimensional tensile strength from 24 hours of hydration and onwards. The obtained development of the modulus of elasticity in tension has been compared with the development in compression and the results indicate that they are equal, see Fig. 3.27 and 3.28.

The tensile strength development has been measured and the splitting tensile strength has been compared with the one-dimensional strength. The results indicate that the one-dimensional strength exceeds the splitting tensile strength earlier than about 14 days whereas the opposite holds true at later ages when the hydration took place at $20°C$. This shift in behavior has been analysed using finite elements and explained with the development in the Poisson's ratio. At $40°C$ of hydration the conclusion is not as clear due to measurement problems.

Application of the maturity transformation has been found to describe the development of modulus of elasticity and the strength satisfactory. However, some discrepencies are observed but it is assumed that they are mainly due the above mentioned problems.

The magnitude of creep in the tensile experiments was found to be comparable to the magnitude in compression. This indicate that the creep properties measured in compressive experiments may be used in the analysis where tensile creep phenomena occur. Further the non-linearity observed in compressive creep experiments reported in the literature for high stress levels was also observed in the present creep experiments in tension.

The influence from temperature gradients in time on the magnitude of creep was found to be significant. The observed creep increased significantly when gradients appeared. For different constant temperature levels the conclusions based on the experiments carried out are not as clear.

The relaxation is significant even when the concrete is loaded after 72 hours of hydration at $20°C$. After about 120 hours the stress level was decreased to 50% of the initial value.

Bibliography

[1] Al-Kubaisy, M.A. and Young, A.G., (1975). *Failure of Concrete under Sustained Tension*, Magazine of Concrete Research, Vol. 27, No. 92.

[2] ASTM Designation: C 496–85, *Standard Test Method for Splitting Tensile Strength of Cylindrical Concrete Specimens*, 1985.

[3] Bažant, Z.P., ed. (1988). *Mathematical modeling of creep and shrinkage of concrete.* John Wiley, New York, N.Y.

[4] Byfors, J. (1980). *Plain Concrete at Early Ages*, CBI Forskning, Research 3:80, Swedish Council for Building Research.

[5] CIMS-2D manual (1994), in danish. DTI, The Institute of Buildingtechnology.

[6] COSMOS manual (1993). Version 1.70.

[7] Dahlblom, O. and Ottosen, N.S. (1987). *Smeared Crack Analysis Using Generalized Fictitious Crack Model*, Journal of Engineering Mechanics, Vol. 116, No. 4.

[8] Fosroc, Nitomortar PE, (1993). *High strength jointing and multi-purpose repair compounds*, Nitomortar PE CI/SfB: (4-) Pr4.

[9] *HETEK phase 4, Material Modelling, Continuum Approach.*

[10] Herholdt, AA.D., Justesen, Chr. F.P., Nepper-Christensen, P. og Nielsen, A., (1985). *The Concrete bool*, in danish, 2. ed., The technical information center of the cement-producers, Aalborg, Denmark.

[11] Jensen, O.M., et al., (1996). *HETEK phase 2, Shrinkage of Concrete.*

[12] Mehta, P.K., and Monteiro, P.J.M., (1993). *Concrete, Structure, Properties and Materials*, Prentice Hall, Englewood Cliffs, 2. ed.

[13] Neville, A.M., Dilger, W.H. og Brooks, J.J. (1983). *Creep of plain and structural concrete*, Construction Press, London and New York.

[14] Nielsen, A. (1972). *Rheology of Building Materials*, National Swedish Building Research, Document D6.

[15] Rüsch, H. (1960). *Researches toward a general flexural theory for structural concrete* Proceedings for the American Concrete Institute, Vol. 57, No. 1, pp. 1–28.

[16] Schutter, G. De and Taerwe, L., (1996). *Degree of hydration-based description of mechanical properties of early age concrete*, Materials and Structures, Vol. 29, p. 335.

[17] Spange, H. and Pedersen, E.S., (1996). *HETEK, Control of Early Age Cracking, Phase 1: Early Age Properties of Selected Concrete*, Report No. xx, The danish road directorate.

[18] Umehara, H., Uehara, T., Iisaka, T. and Sugiyama, A., (1994). *Effect of creep in concrete at early ages on thermal stress*, Proc. of the RILEM Symposium on Thermal Cracking in Concrete at Early Ages, Münich, Ed. R. Springenschmid.

[19] The standard for testing of hardened concrete from the danish engineer association, *Testing of Concrete – Making and curing of moulded test specimens for strength tests*, in danish, DS 423.21, Copenhagen, Denmark.

[20] The standard for testing of hardened concrete from the danish engineer association, *Testing of Concrete – Hardened Concrete, Compressive Strength*, in danish, DS 423.23, Copenhagen, Denmark.

[21] The standard for testing of hardened concrete from the danish engineer association, *Testing of Concrete – Hardened Concrete, Tensile Strength*, in danish, DS 423.24, Copenhagen, Denmark.

[22] The standard for testing of hardened concrete from the danish engineer association, *Testing of Concrete – Hardened Concrete, Modulus of Elasticity*, in danish, DS 423.25, Copenhagen, Denmark.

Appendix A

Appendix

A.1 Tensile strength and modulus of elasticity at 20°C.

Age, Hours	Specimen	f_t, MPa	E_{lower}, GPa	E_{upper}, GPa
25.3	1	1.41	27.1	28.2
25.9	2	1.38	25.4	25.3
26.2	3	1.31	27.9	27.4
Mean		1.37	26.8	27.0
69.0	1	1.91	35.2	37.9
69.5	2	1.76	33.2	34.5
70.0	3	1.94	36.2	36.7
Mean		1.87	34.9	36.3
169.0	1	2.16	34.7	36.2
169.5	2	1.87	36.7	33.9
170.0	3	2.15	33.8	34.5
Mean		2.06	35.1	34.9
-	-	-	-	-
358.0	2	2.56	40.6	38.1
358.5	3	2.30	37.8	36.0
Mean		2.43	39.2	37.1
-	-	-	-	-
699.0	2	3.21	41.4	44.7
699.5	3	3.11	42.4	42.8
Mean		3.16	41.9	43.8

A.2 Splitting tensile strength at 20°C.

Age, Hours	Specimen	f_sp, MPa
19.2	1	0.65
19.3	2	0.87
19.3	3	0.62
Mean		0.71
46.0	1	1.87
46.1	2	1.75
46.2	3	1.47
Mean		1.70
71.0	1	1.92
71.1	2	2.24
71.2	3	2.29
Mean		2.15
168.0	1	2.60
168.1	2	2.07
168.2	3	2.25
Mean		2.31
336.0	1	2.87
336.1	2	2.86
336.2	3	2.55
Mean		2.76
672.0	1	4.02
672.1	2	3.40
672.2	3	3.30
Mean		3.57

A.3 Tensile strength and modulus of elasticity at $40°C$.

Age, Hours	Specimen	f_t, MPa	E_{lower}, GPa	E_{upper}, GPa
24.0	1	1.36	22.7	23.9
24.8	2	1.57	20.9	26.1
25.8	3	1.53	25.1	24.5
Mean		1.485	22.9	24.8
44.5	1	2.29	32.2	32.6
45.3	2	1.91	35.7	37.9
46.0	3	2.34	34.6	35.0
Mean		2.18	34.2	35.2
49.7	1	2.31	38.5	39.9
50.3	2	2.50	41.0	38.7
51.5	3	2.04	45.1	41.9
Mean		2.28	41.5	40.2
70.5	1	2.50	36.7	39.0
72.0	2	2.72	39.5	42.1
73.0	3	2.28	38.9	40.7
Mean		2.50	38.4	40.6
168.0	1	3.02	43.5	45.3
169.0	2	3.07	40.9	41.6
170.0	3	3.07	44.8	46.4
Mean		3.05	43.1	44.4
-	1	-	-	-
337.0	2	3.42	41.3	41.6
338.0	3	3.28	40.0	43.1
Mean		3.35	40.7	42.4
697.0	1	4.42	50.4	49.7
697.5	2	4.15	43.0	43.1
698.0	3	4.00	42.7	43.4
Mean		4.19	45.4	45.4

A.4 Splitting tensile strength at $40°C$.

Age, Hours	Specimen	f_sp, MPa
19.2	1	0.57
19.3	2	0.58
19.3	3	0.59
Mean		0.58
25.0	1	1.08
25.1	2	1.41
25.2	3	1.42
Mean		1.30
43.0	1	2.21
43.1	2	1.87
43.2	3	1.64
Mean		1.91
76.0	1	3.05
76.1	2	2.52
76.2	3	2.57
Mean		2.71
144.0	1	3.48
144.1	2	2.77
144.2	3	3.14
Mean		3.13
312.0	1	3.15
312.1	2	3.42
312.2	3	3.30
Mean		3.29
672.0	1	3.92
672.1	2	4.40
672.2	3	4.76
Mean		4.36

Appendix B

Appendix

B.1 Compressive strength and modulus of elasticity at 20°C.

Age, Hours	Specimen	f_c, MPa	E, GPa
18.0	1	4.01	13.2
18.0	2	4.08	11.1
18.0	3	4.08	13.9
Mean		4.06	12.7
48.0	1	17.3	24.5
48.0	2	18.7	27.1
48.0	3	17.5	24.4
Mean		17.8	25.3
72.0	1	22.6	25.8
72.0	2	21.7	30.0
72.0	3	24.3	30.5
Mean		22.9	28.8
168.0	1	-	32.9
168.0	2	25.7	33.6
168.0	3	27.0	36.3
Mean		26.3	34.3
336.0	1	27.9	34.5
336.0	2	33.0	35.9
336.0	3	29.1	37.0
Mean		30.0	35.8
672.0	1	37.3	-
672.0	2	33.4	-
672.0	3	33.5	38.2
Mean		34.7	38.2

B.2 Compressive strength and modulus of elasticity at $40°C$.

Age, Hours	Specimen	f_c, MPa	E, GPa
18.0	1	4.59	14.7
18.0	2	4.84	14.6
18.0	3	4.65	14.9
Mean		4.69	14.7
30.5	1	17.8	24.3
30.5	2	17.9	27.2
30.5	3	17.1	-
Mean		17.6	25.7
40.5	1	24.2	35.1
40.5	2	20.2	32.3
40.5	3	20.2	29.2
Mean		21.5	32.2
80.5	1	30.0	33.5
80.5	2	29.2	33.8
80.5	3	30.3	34.7
Mean		29.8	34.0
150.5	1	34.8	-
150.5	2	31.2	36.5
150.5	3	-	38.1
Mean		33.0	37.3
290.5	1	40.1	37.2
290.5	2	42.7	36.9
290.5	3	41.5	37.9
Mean		41.4	37.3

Appendix C

Appendix

C.1 Measured creep in Tension, Age at Loading 1 day

C.1.1 40% Load level, Creep vs. Time, Specimen 1

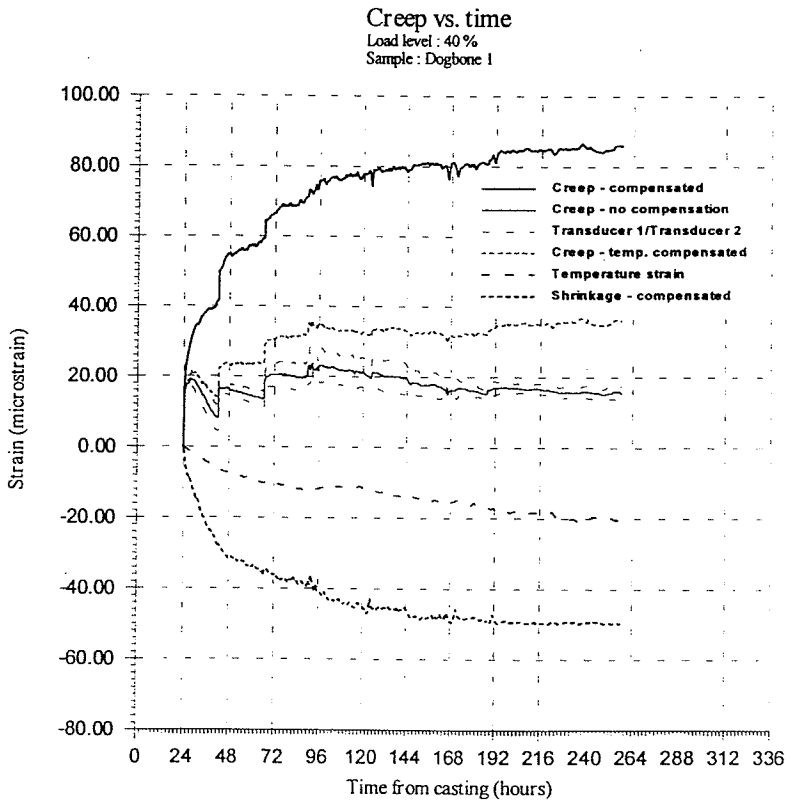

C.1.2 40% Load level, Creep vs. Time, Specimen 2

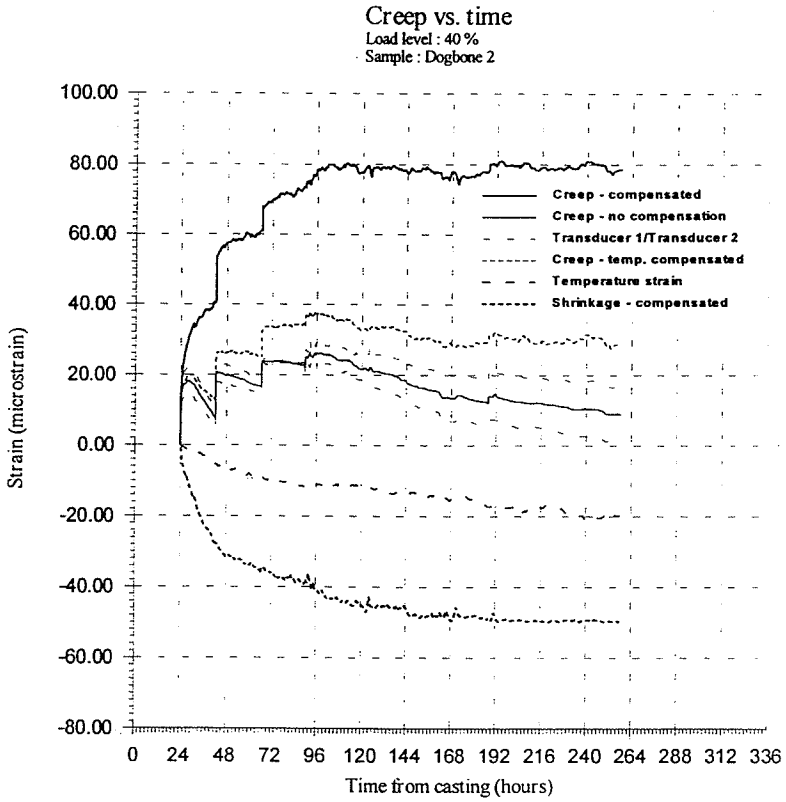

C.1.3 40% Load level, Shrinkage and Temperature vs. Time

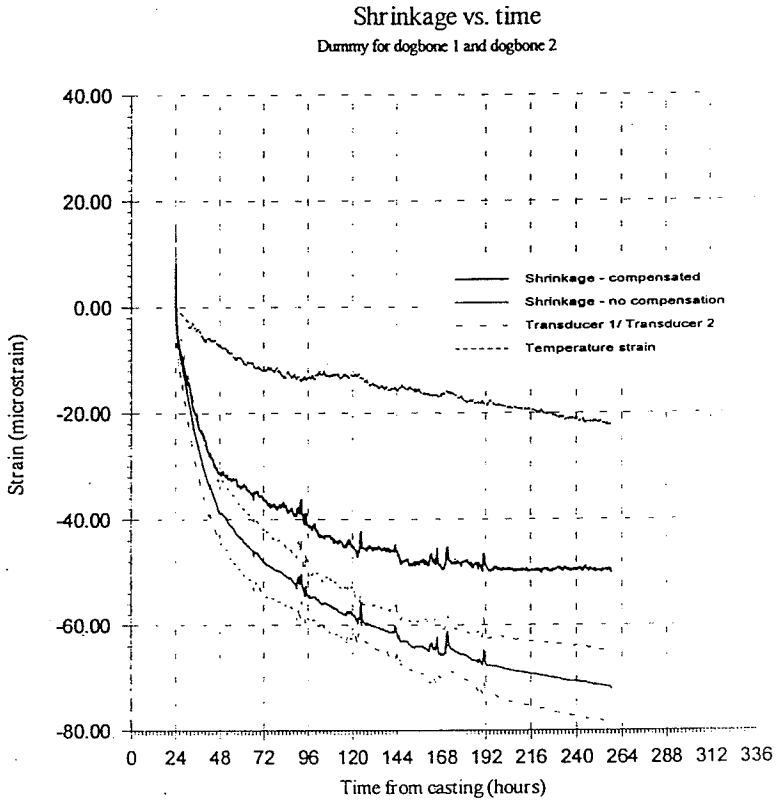

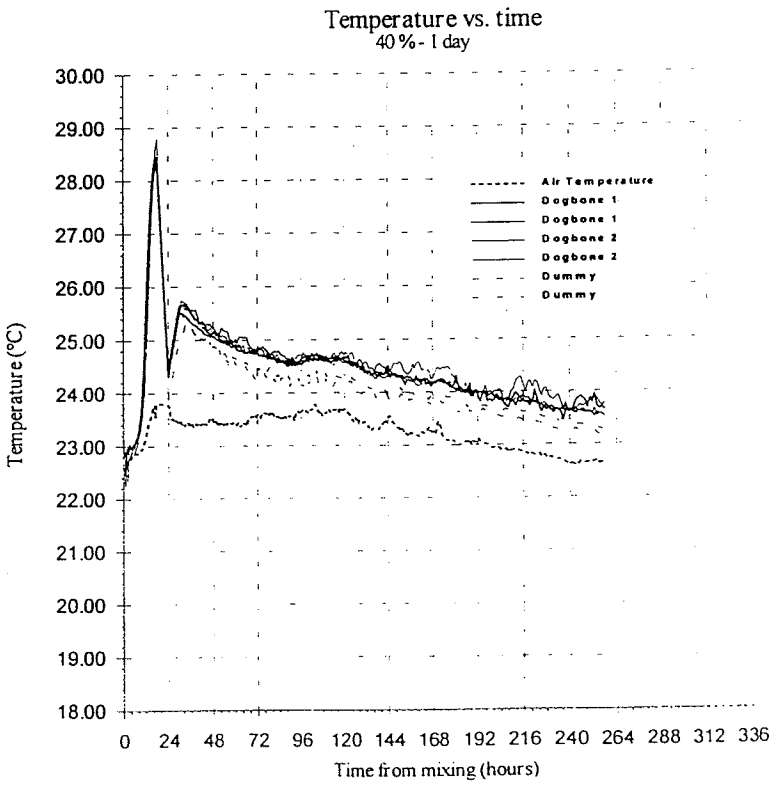

C.1.4 60% Load level, Creep vs. Time, Specimen 1 and 2

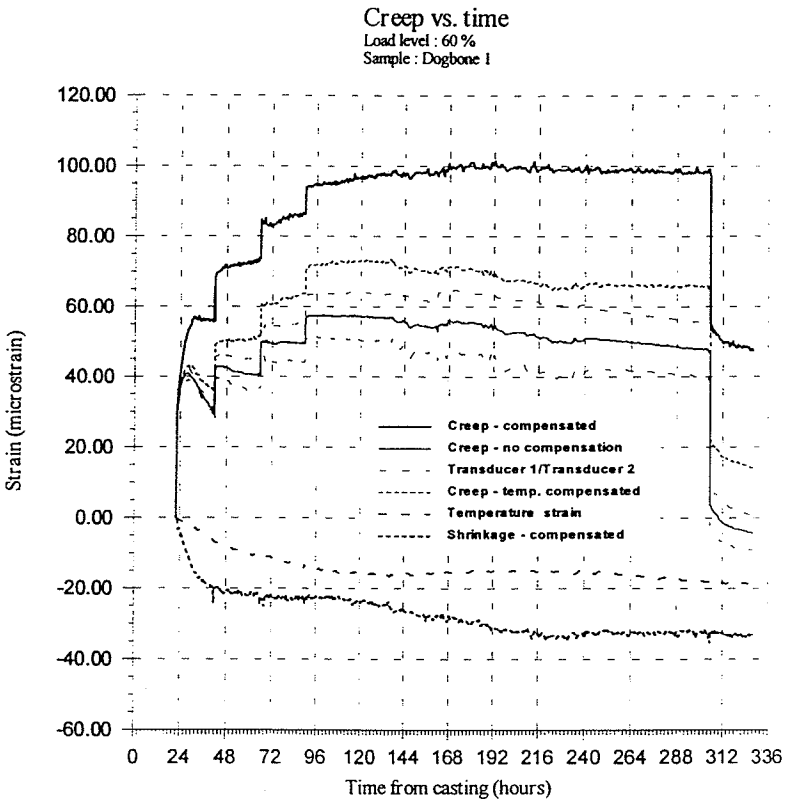

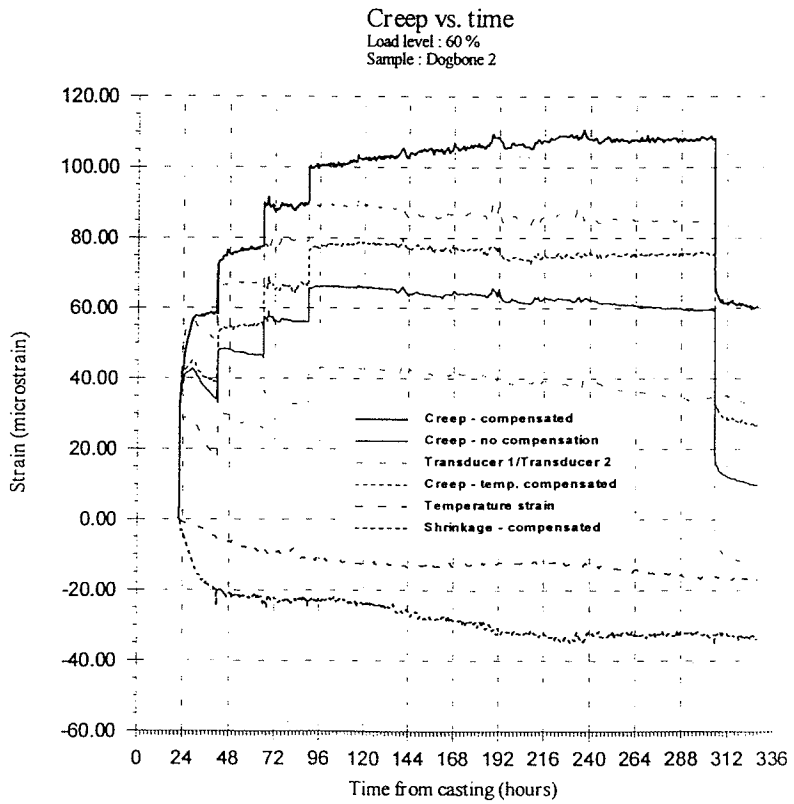

C.1.5 60% Load level, Shrinkage and Temperature vs. Time

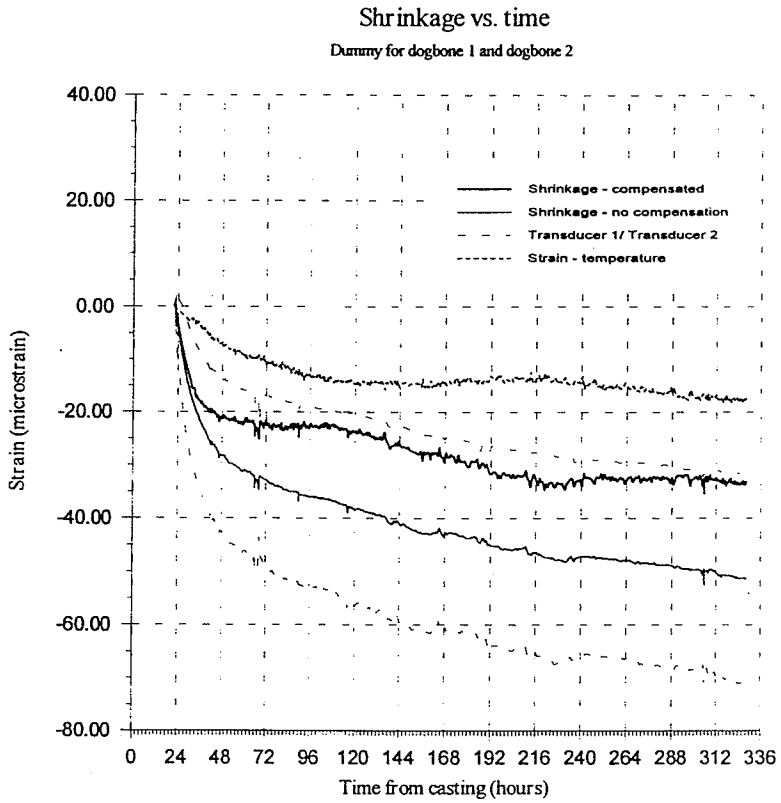

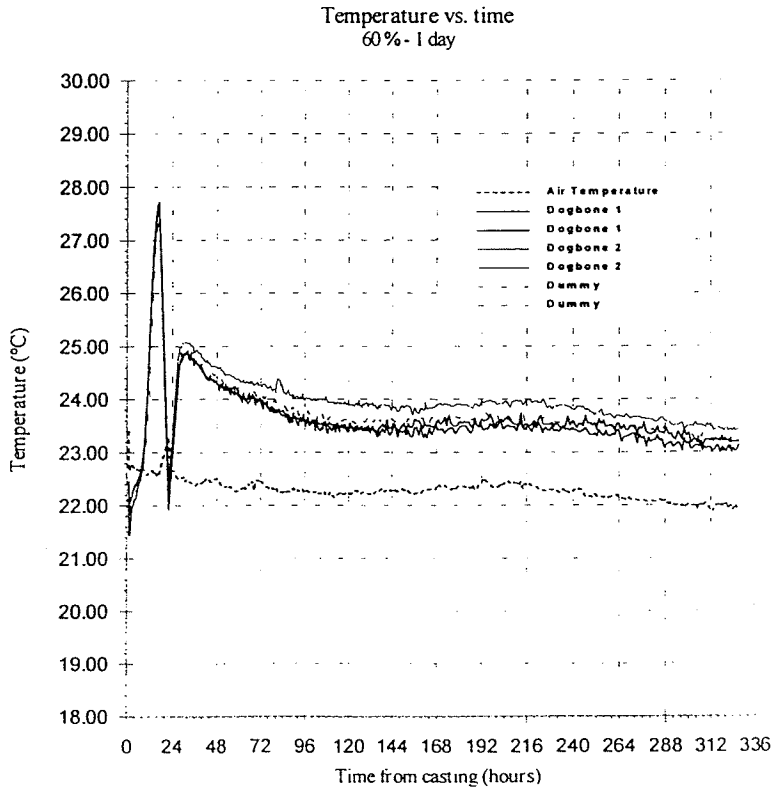

C.1.6 80% Load level, Creep vs. Time, Specimen 2

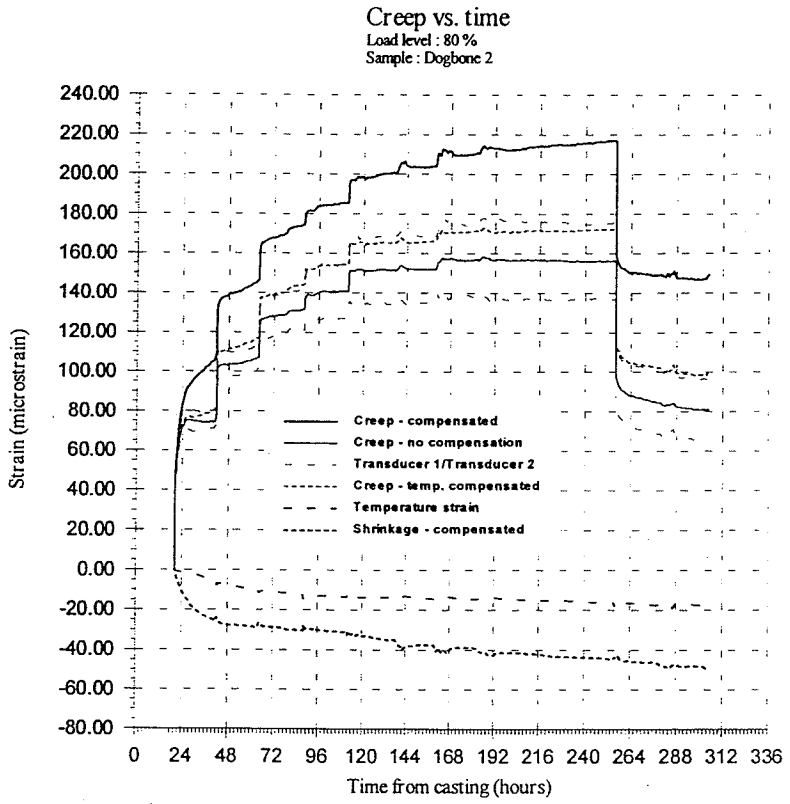

C.1.7 80% Load level, Shrinkage and Temperature vs. Time

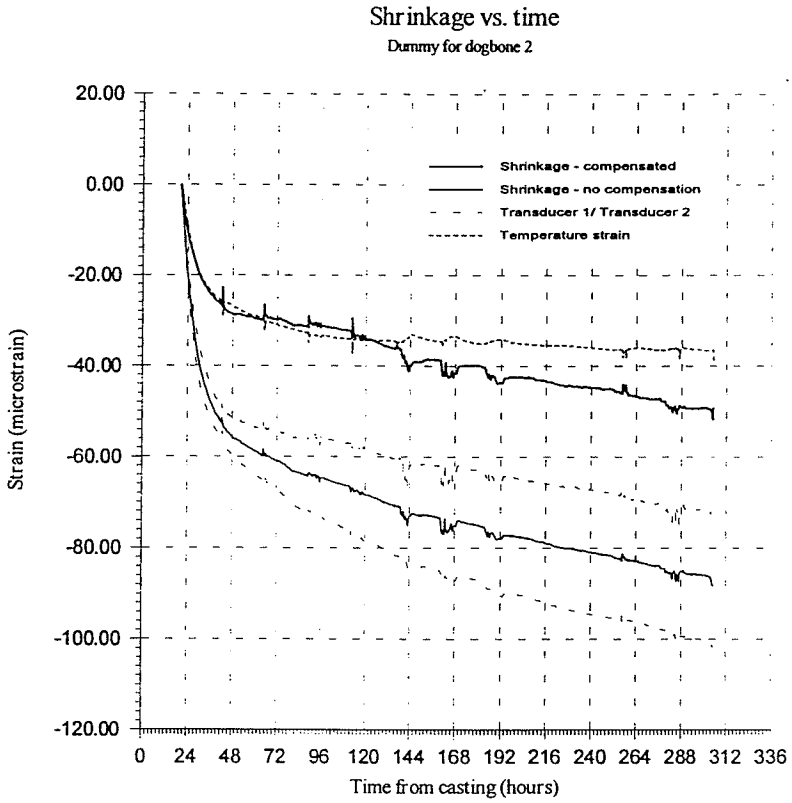

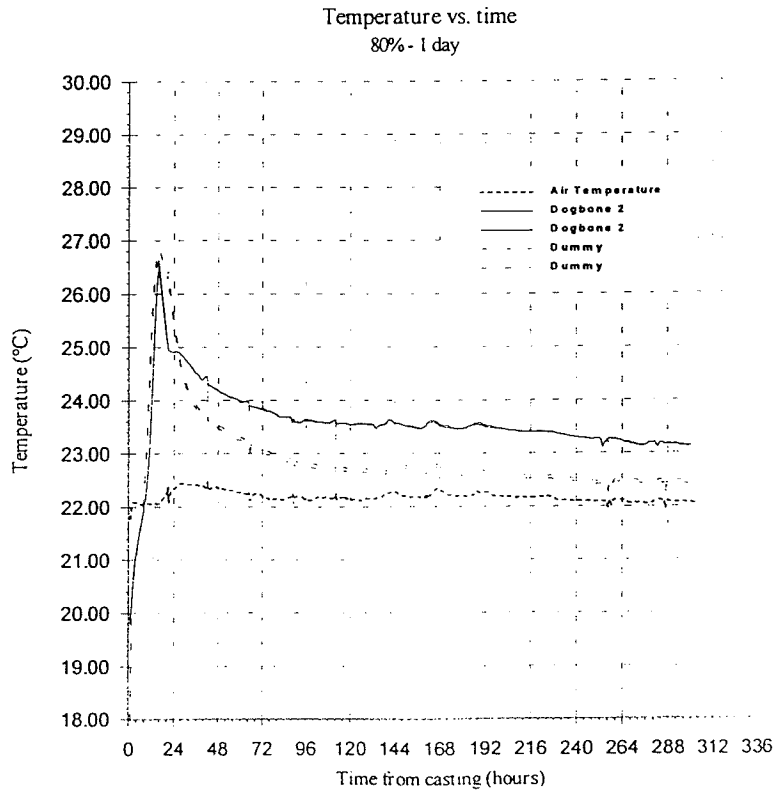

C.2 Measured creep in Tension, Age at Loading 3 day

C.2.1 40% Load level, Creep vs. Time, Specimen 1 and 2

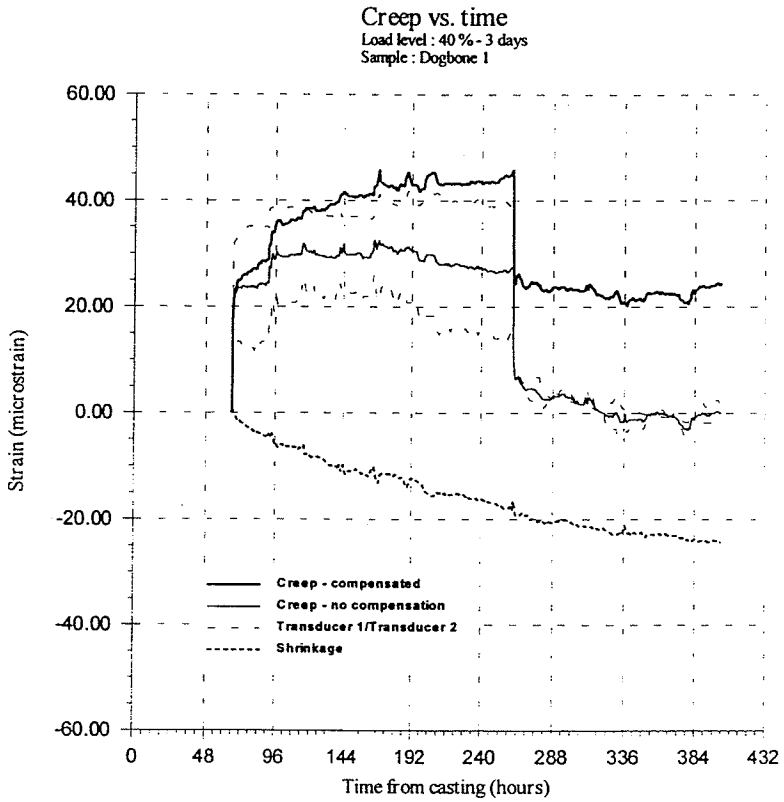

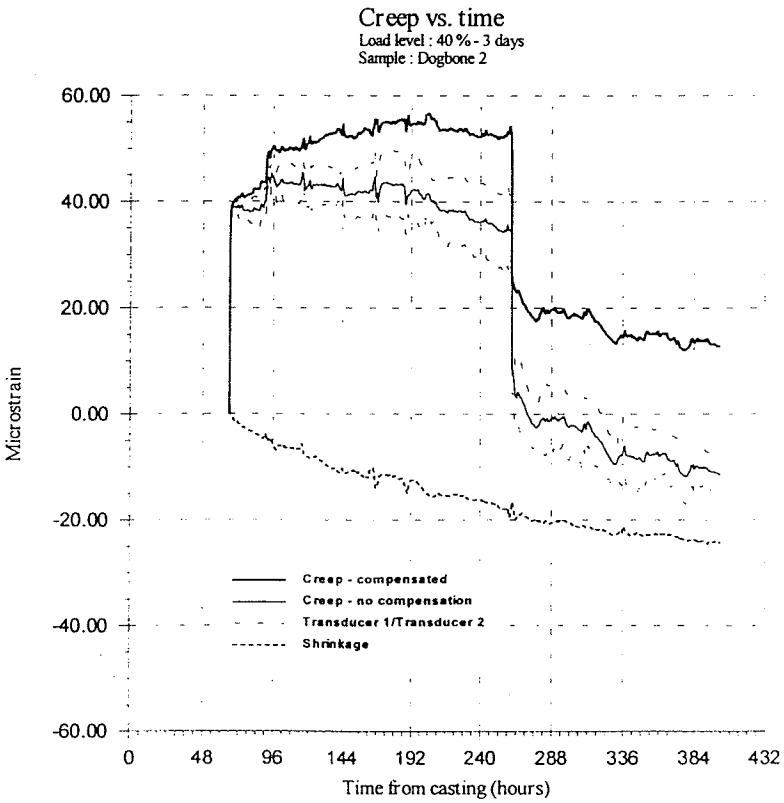

C.2.2 40% Load level, Shrinkage and Temperature vs. Time

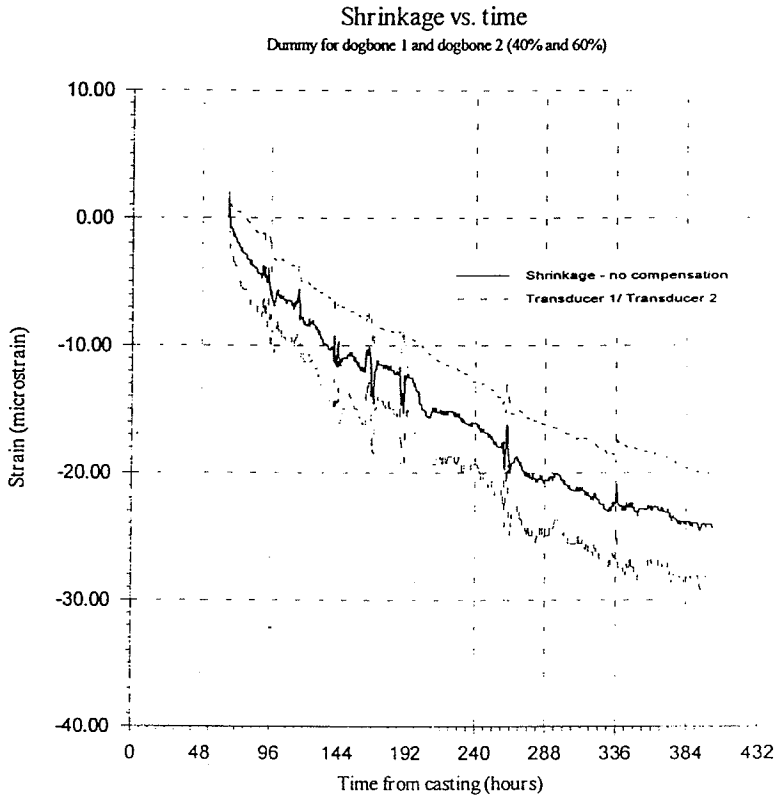

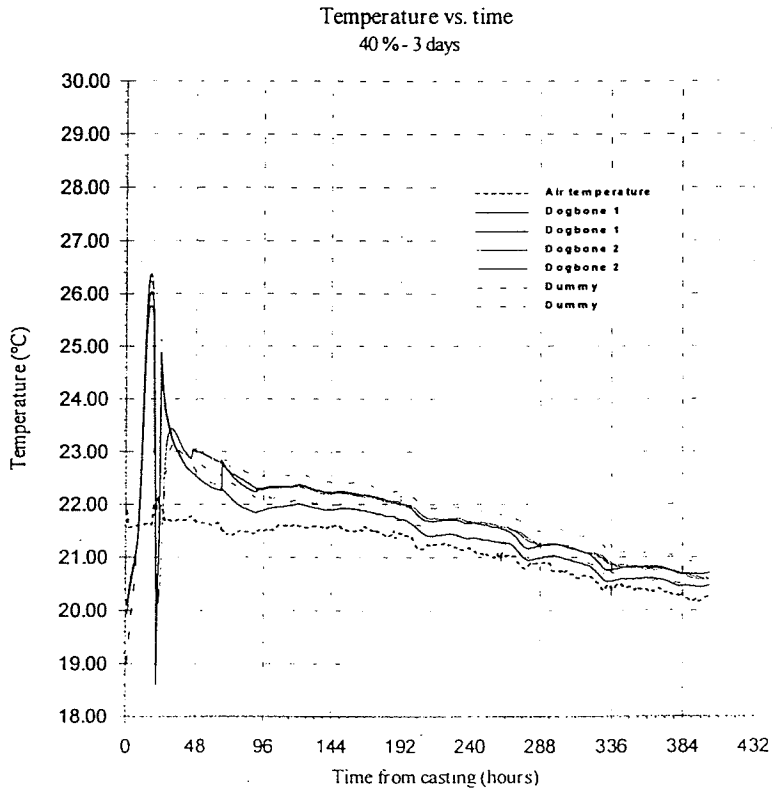

C.2.3 60% Load level, Creep vs. Time, Specimen 1 and 2

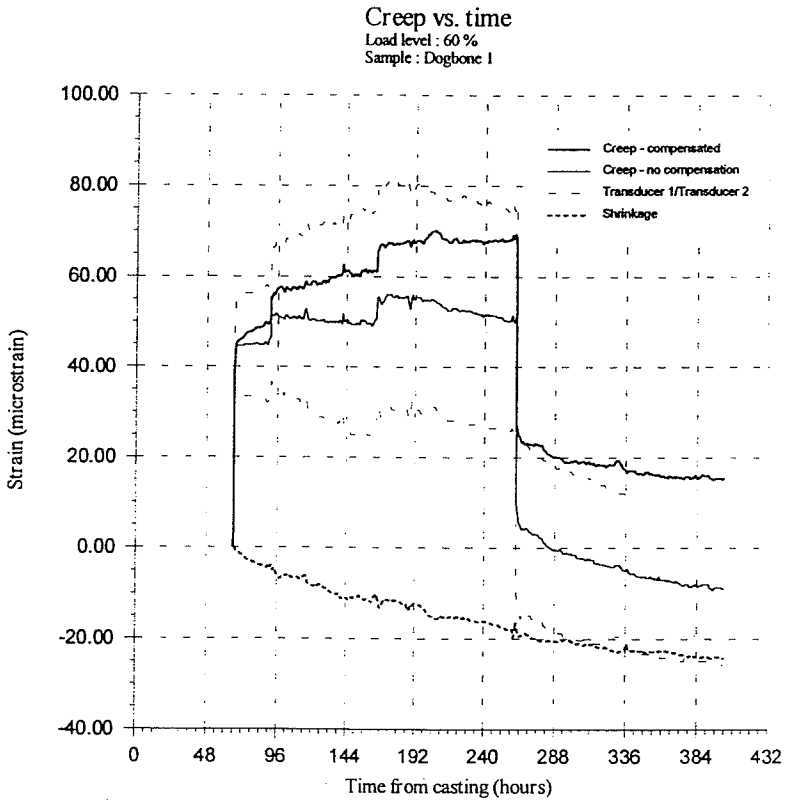

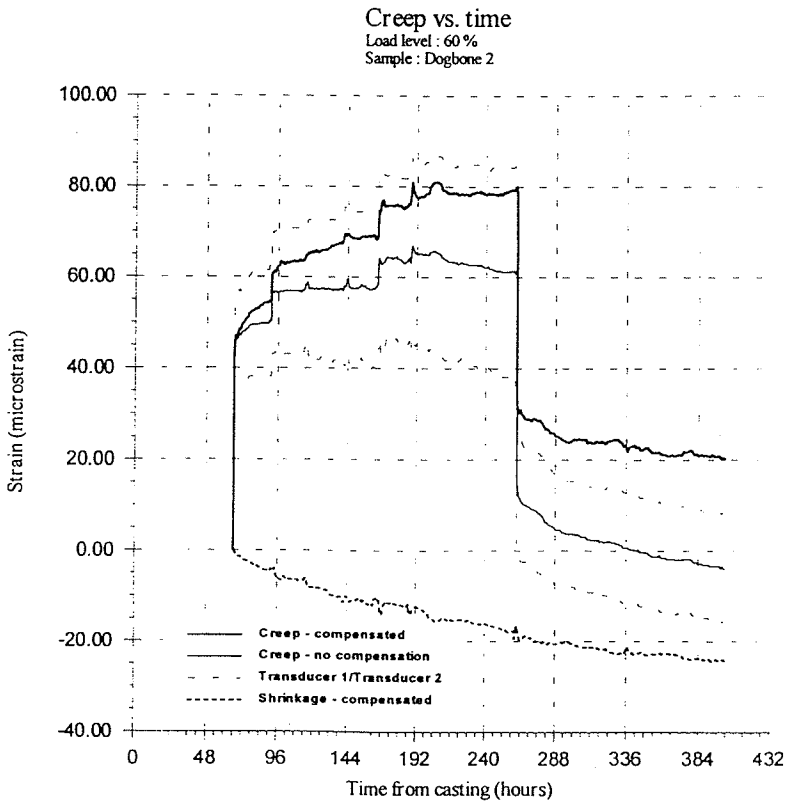

C.2.4 60% Load level, Shrinkage and Temperature vs. Time

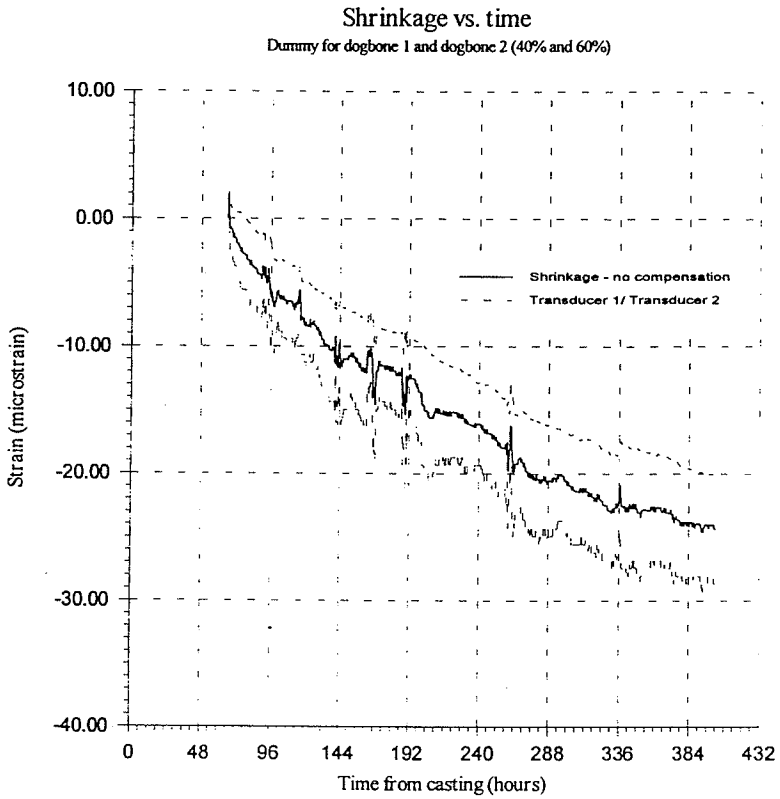

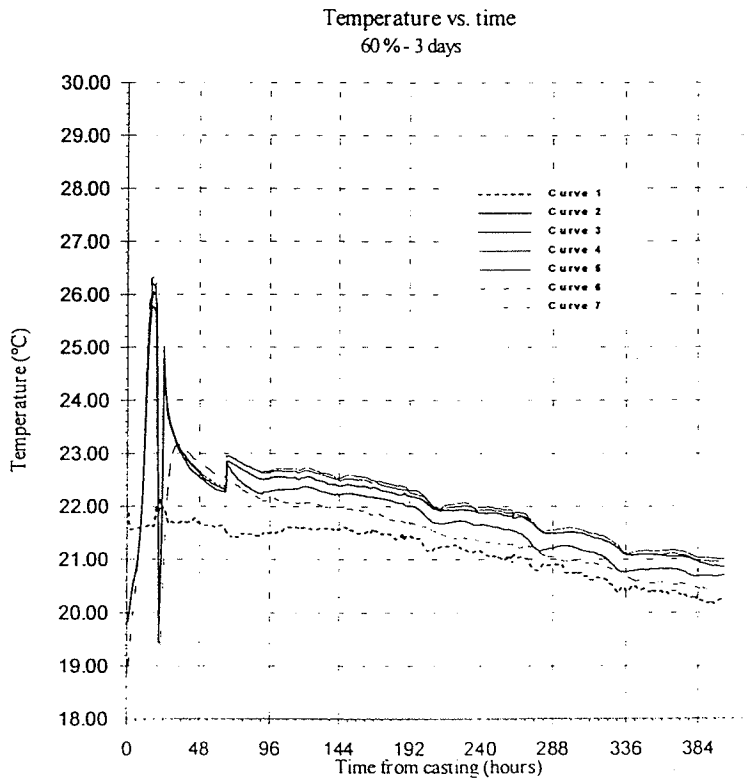

Appendix D

Appendix

D.1 Measured creep in Compression

D.1.1 40% Load level, 24°C, Creep and Shrinkage vs. Time

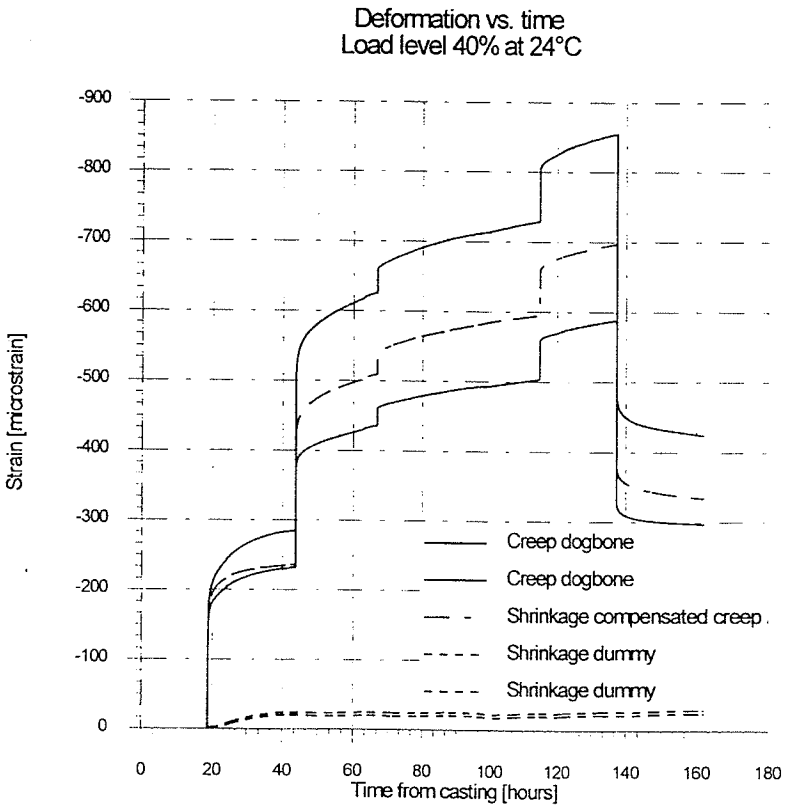

D.1.2 40% Load level, 24°C, Temperature vs. Time

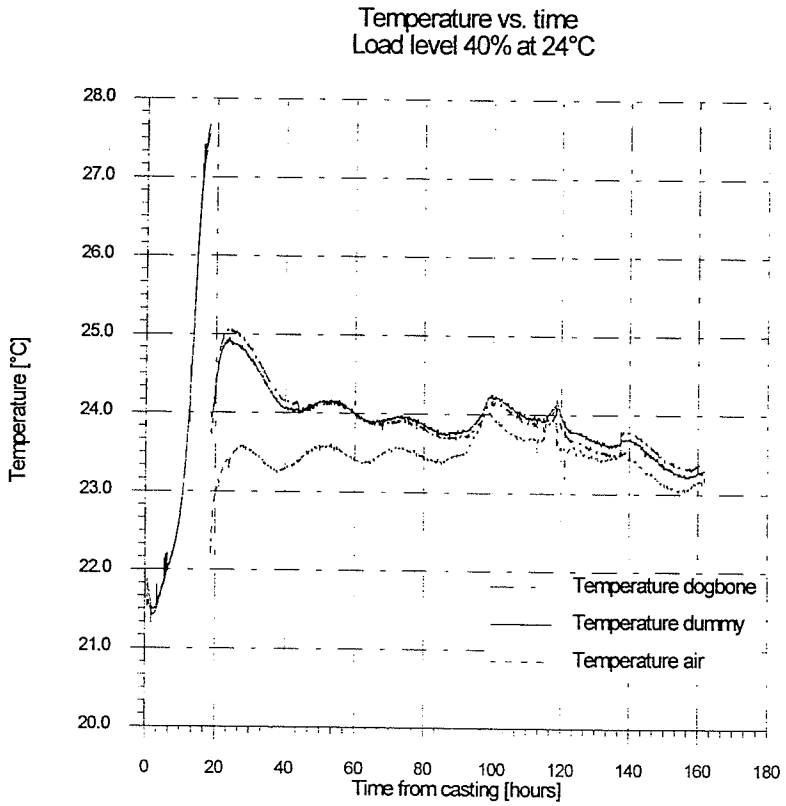

D.1.3 40% Load level, 40°C, Creep, Shrinkage and Temperature vs. Time

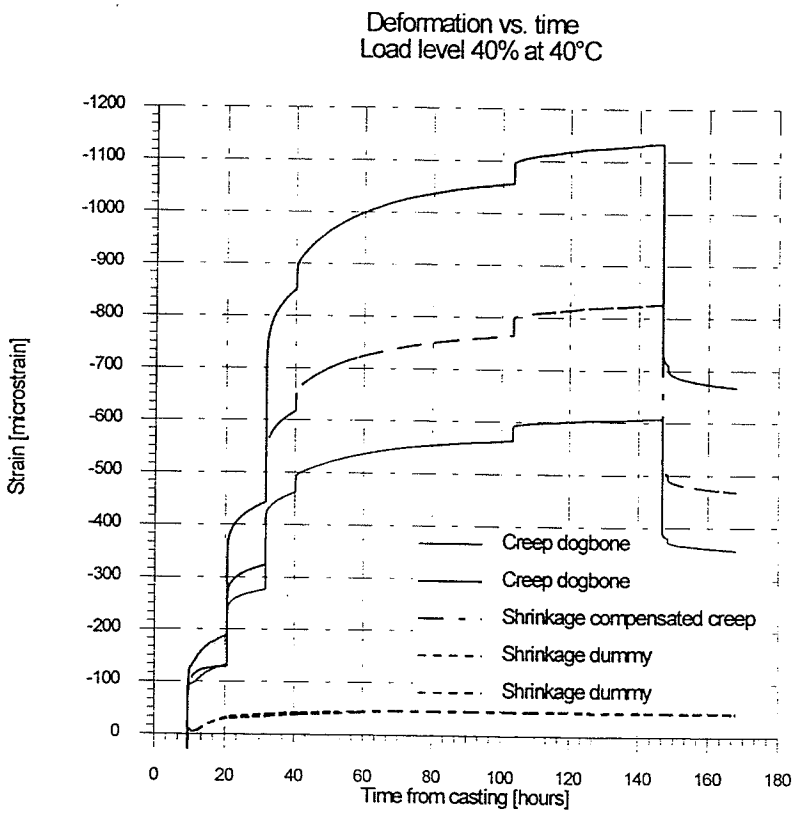

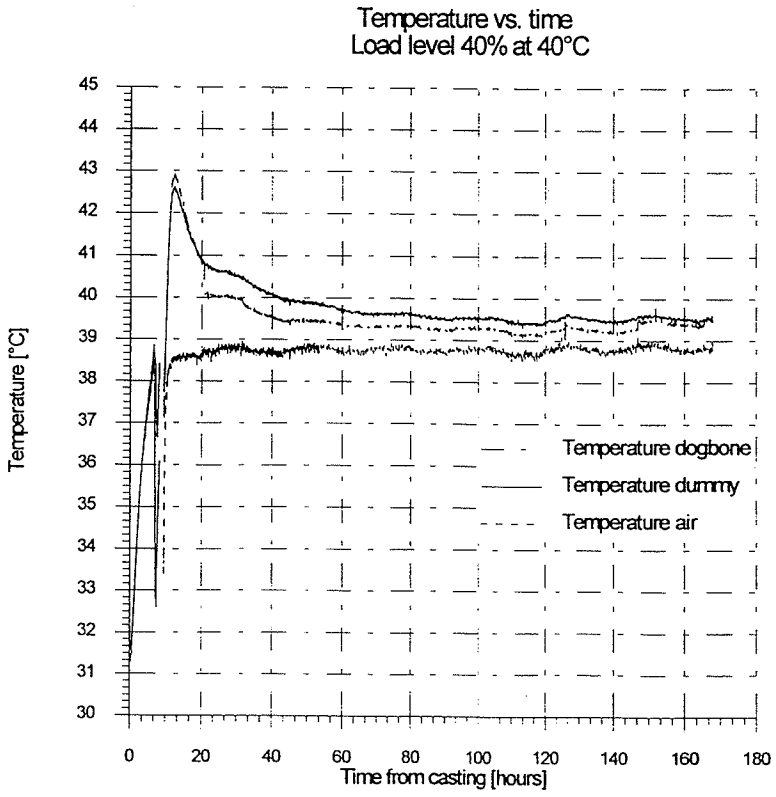

D.1.4 40% Load level, 20-40-20°C, Creep, Shrinkage and Temperature vs. Time

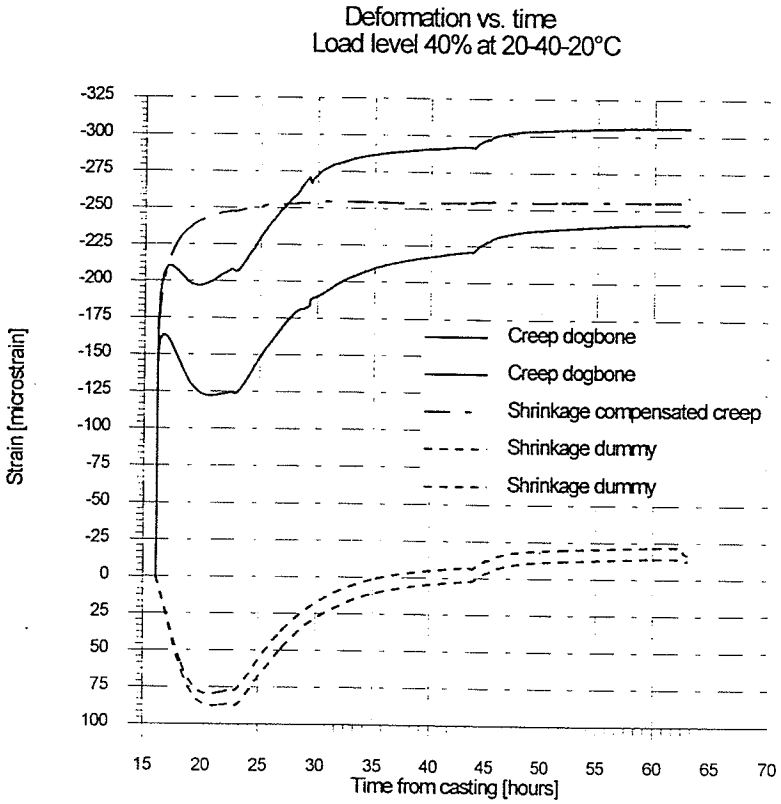

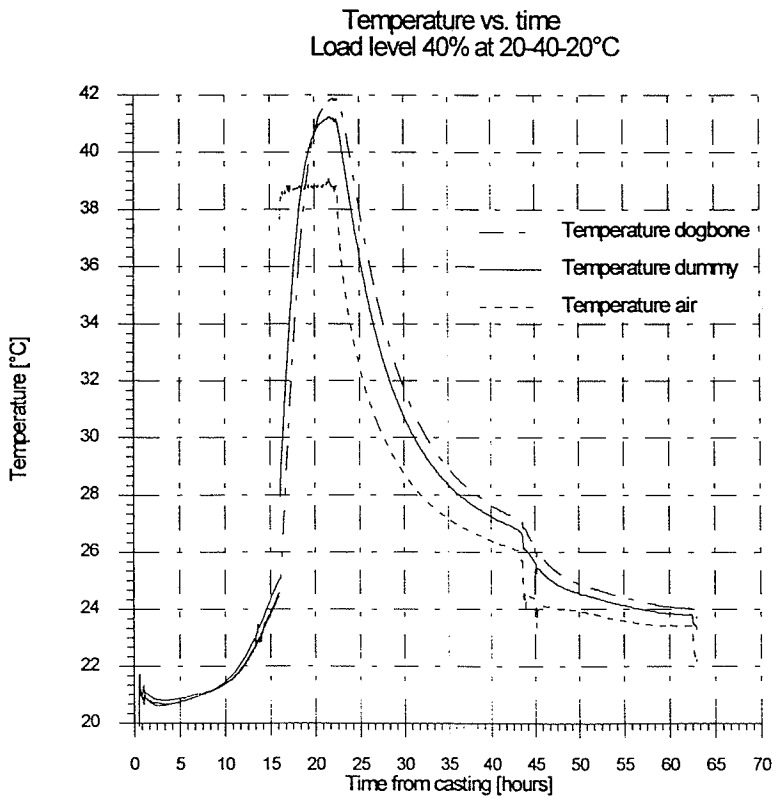

Appendix E

Appendix

E.1 Experimental Program on Creep in Tension

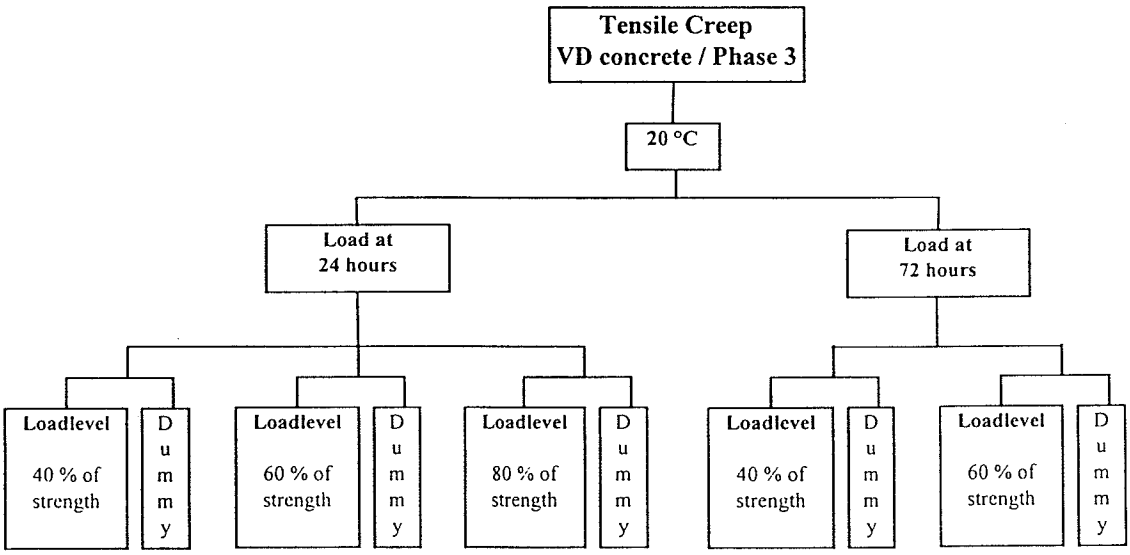

E.2 Experimental Program on Creep in Compression